UNIVERSITÀ DEGLI STUDI DI MILANO

Facoltà di Medicina e Chirurgia

Dottorato di Ricerca in Scienze Morfologiche XXIII Ciclo

BIO16

THREE-DIMENSIONAL FACIAL ANTHROPOMETRY

Coordinatore: Chiar.ma Prof.ssa Magda Gioia

Tutor: Chiar.ma Prof.ssa Chiarella Sforza

Tesi di Dottorato di

Márcio de Menezes

Matr. Nr. R07929

Anno Accademico 2009/2010

CONTENTS

Acknowledgements 1

Abstract 2

1. Introduction 3

1.1 Methods for developing applications 3

1.1a Facial landmarks 3

1.1b Three-dimensional image analyzers 4

1.1c Statistical Methods errors 7

1.2 Aim 9

2. Study 1- A photographic system for the three-dimensional study of facial morphology 10

2.1 Materials and methods 10

2.2 Results 12

2.3 Discussion 13

2.4 Conclusion 14

3. Study 2 - Accuracy and reproducibility of a 3d stereophotogrammetric imaging system 15

3.1 Materials and methods 15

3.2 Results 17

3.3 Discussion 18

3.4 Conclusion 20

4. Study 3- Digital dental cast placement in 3-dimensional, full-face reconstruction: A technical evaluation 21

4.1 Materials and methods 21

4.2 Results 24

4.3 Discussion 24

4.4 Conclusion 25

5. Study 4 - Unilateral cleft lip and palate (UCLP): a 3D evaluation 26

5.1 Materials and methods 26

5.2 Results 28

5.3 Discussion 28

5.4 Conclusion 30

6. General conclusion 31

7. References 32

8. Webography 37

9. Figures 38

10. Tables 48

ACKNOWLEDGEMENTS

Though my life I have learned one thing: I could never have done anything without the support and encouragement of a lot of people. First, I would like to thank my advisor, Prof.ssa Chiarella Sforza. You've been my mentor, my confidant, my colleague, and a never-ending fount of patient and scientific knowledge. You have given so much of yourself to help me succeed. If I do take the academic path, I only hope that I can be half the advisor that you have been to me. Whatever path I do take, certainly I learned a lot because of you.

I owe my deepest gratitude to all professors, researchers, colleagues and member of my department. I have learned so much from all of you. Especially thanks to Dr. Riccardo Rosati, Dr. Andrea Mapelli, Salvatore Sergi (Mimmo), your friendship and collaboration have been tremendous throughout my Ph.D.

I would like to show my gratitude to Prof. Marco Antonio Moreira Rodrigues da Silva, who have helped me on my way here and also during my time at the Restorative Dentistry Department (FORP - USP), where I learnt a great deal from all of the people there. I also have to thank the Prof(a) Claúdia Maria de Felício who shared her experience, providing me with helpful advice and assistance.

This period of work and living abroad would not have been possible without the support of my best friend, Ahmed Aufy. You're always there for me, when I need help or moral support. You're a person I turn to in good times and in bad. You have given me the courage to make the next transitions in my life. For all of this, I thank you.

I convey special acknowledgement and my profound appreciation to my girlfriend for her supportive, encouraging, understanding, and patience even during hard times of this study. Thank you.

Where would I be without my family? My parents deserve special mention for their inseparable support and prayers. Thus, I would like to dedicate this work to my family: Tércio, Marlene, Marcel and Maico. Without your unending support and love from childhood to now, I never would have made it through this process or any of the tough times in my life. Thank you.

Finally, I would like to thank everybody who was important to the successful realization of thesis, as well as expressing my apology that I could not mention personally one by one.

ABSTRACT

The use of 3D surface technology is progressively increasing in health clinics and research centers. Methods of capturing 3D facial surface may obtain more imaging information providing a reliable and fast analysis. Stereophotogrammetry is a promising method of soft-tissue evaluation that allows reliable analysis of craniofacial deformities, providing fundamental parameters to plan and evaluate dental treatments and maxillofacial surgery, so improving the multi-disciplinary and multi-species studies of genotype–phenotype correlations through simple and precise measurements.

In the current study, photogrammetry/stereophotogrammetry systems were used to evaluate soft-tissue facial morphology and dental casts. Three-dimensional images were collected and rebuilt in 3D, using software for rendering images to establish, analyze and compare morphology features of craniofacial structures, and to assess the usage and limitations of these devices. The use and investigation of this system were divided in 4 studies: 1) A photographic system for the three-dimensional study of facial morphology; 2) Accuracy and reproducibility of a 3D stereophotogrammetry imaging system; 3) Digital dental cast placement in 3-dimensional, full-face reconstruction: A technical evaluation and 4) Unilateral Cleft Lip and Palate (UCLP): a 3D evaluation.

The current studies found the used 3D image systems both accurate and repeatable. The 3D devices and the methods analyzed in these studies could therefore be usefully used for clinical analysis in maxillofacial, plastic and esthetic surgery, as well as in all dental fields. The 3D stereophotogrammetric systems have several advantages over direct anthropometry and gradually are becoming into more accessible cost, replacing classical methods to quantify surface topography.

Key Words: Three-dimensional analysis, stereophotogrammetry, 3D surface imaging technology, anthropometry

1. INTRODUCTION

One of the oldest methods of examination, still being used in medicine, is Anthroposcopy, which consists in a form of anthropology based upon visual observation of the characteristics of the human body. In contrast, Anthropometry is a systematic quantitative representation of the human body, used to measure the absolute and relative variability in size and shape[1]. Both procedures are essential to the medical field, especially anthropometric measurements of the head and face, with a significant change in the process of diagnosis for various syndromes, giving support to plastic and orthognathic surgery, detecting normal and abnormal growth, and providing information for planning and evaluating medical procedures and treatments.

Classic direct anthropometry has greatly helped clinicians in the past [2], but presently the advent of digital techniques for the imaging of the facial skeleton should be met by some new methods for soft-tissue facial imaging and measurement. In clinical investigations and research, classic direct anthropometry is being coupled and even replaced with various three-dimensional image analyzers. With a great clinical implication, methods or techniques for 3D imaging evaluation might be reaching the optimum for the diagnostic and therapeutic information.

Fundamentally, digital anthropometry collects a set of digital landmarks from the soft-tissue surface, and uses their spatial x, y, z coordinates as end-points for calculations based on Euclidean geometry: linear distances and angles similar to those provided by conventional anthropometry are computed.

1.1 Methods for Developing Applications

In this section, we examine instruments, protocols and method used along this thesis to expose the kinds of support necessary for the performed studies.

1.1a Facial Landmarks

After the identification of facial anatomical landmarks, classic direct anthropometry makes measurements over them, using calipers, protractors or other instruments[2]. Basically, anatomical landmarks represent not only the linkage between classic direct anthropometry and digital anthropometry, but also increase the level of precision of digital assessments, thus providing a fairly good congruence with traditional anthropometry[3].Digital anthropometry collects a set of digital

landmarks from the soft-tissue surface, and using Euclidean geometry, measurements can be done through x, y, z coordinates[4].

Regarding the anatomical landmarks and the qualitative and quantitative evaluation of the facial soft tissues, in our lab we used 50 landmarks[2, 5] that can describe the main facial features (Figure 1).

- midline landmarks: Tr, trichion; G, glabella; N, nasion; PrN, pronasale; C', columella; SN, SubNasale; Ls, labiale superius; Sto, stomion; Li, labiale inferius; Sl, sublabiale; Pg, pogonion; Me, menton;

- paired landmarks (right and left side noted r and l): Exr, Exl, exocanthion; Enr, Enl, endocanthion; Osr, Osl, orbitale superius; Orr, Orl, orbitale; Ftr, Ftl: frontotemporale; Chkr, Chkl, cheek; Zyr, Zyl, zygion; T*r*, T*l*, tragion; Alr, All, alare; Acr, Acl, nasal alar crest; Itnr, Itnl, inferior point of the nostril axis; Stnr, Stnl, superior point of the nostril axis; Cphr, Cphl, crista philtri; Chr, Chl, cheilion; Gor, Gol, gonion; Prar, Pral, preaurale; Sar, Sal, superaurale; Par, Pal, postaurale; Sbar, Sbal, subaurale.

In the currently protocol used in our laboratory, firstly the landmarks are identified by inspection/palpation, and then are marked with a black eye liner. Subsequent digitization of landmarks is made on the digital images. This protocol allows the use of landmarks that cannot be directly identified on the digital images, such as gonion, thus providing better assessment of facial characteristics.

The reproducibility of landmark identification and marker positioning have previously been reported and found to be reliable, with Dahlberg's errors on 50 landmarks of 1.20 mm for males and 0.95 mm for females, equivalent to 1.04 and 1.05 per cent of the relevant nasion–mid-tragion distances[5, 6].

1.1b Three-dimensional image analyzers

With constant upgrading of informatics and communication technology, the standards for data storage and retrieval and information usage, allied with biomedical knowledge, have transformed traditional methods of diagnosis, visualization, and treatment. These efforts were aimed at reducing the time spent on examinations and improving the reliability of measurements.

Several non-invasive methods are been employed for 3D morphological facial analysis. These instruments can be divided into two main categories: optical, non-contact digitizers, (laser scanners, MRI, optoelectronic instruments, photogrammetry, stereophotogrammetry), and contact instruments (electromagnetic and electromechanical digitizers, ultrasound probes)

Contact instruments

Contact instruments are a precision contact-based desktop 3D digitizing devices, which can be used to measure and capture 3-Dimensional data points from physical objects. The light easy-to-manipulate probe is like a pen that can be used to effortlessly trace objects and capture 3D data. Working on facial morphology acquisition, these devices selected single facial landmarks, providing the coordinates of facial features that directly correspond to anatomical and anthropometric structures [5, 6]

- *Electromechanical*: A mechanical arm rotates around the inside of a cast or the outside of a mold, with mechanical or electromechanical sensors to monitor tip position so that the locations of contact points can be calculated. The cast or mold shape is reconstructed after the entire surface is scanned[4, 7]. (Figure 2)
- *Electromagnetic*: An electromagnetic handheld device contacts the surface of interest, moving within a specified electric field. As it is moved over the surface, the magnet serves as a sensor within the electric field. The position of the sensor in 3-D space is then calculated. An electromagnetic handheld used in this thesis was Polhemus 3Draw, (Polhemus Inc., Colchester, VT) with a resolution of 0.0005 cm/cm of range[4, 5, 8, 9]. (Figure 3)
- *Ultrasound probes*, using acoustic waves in the Megahertz frequency, are widely used for prenatal, intrauterine imaging and diagnosis (Figure 4). This device has been refreshed with a third dimension technology, being able to produce 3D images in real-time allows clinicians to observe and measure the shape and volume of patients' internal anatomy with great detail without using ionizing radiations. New applications within the fields of image guided surgery and radiation therapy are also possible[4, 10]. Ultrasounds are being used to assess the thickness of facial subcutaneous fat in living subjects, thus providing data banks for forensic facial reconstructions that take into account of the effects of sex, age and ethnicity[4, 11, 12].

Optical Instruments

The advantages of optical measurements are a fast data acquisition, non-interaction with the object under test, the possibility of soft tissue measurements. These instruments are used in a wide range of technical and medical applications. The main instruments are laser scanners and stereophotogrammetric systems.

- *Laser Scanners*

The laser scanners are devices capable to emit a laser light and receive the reflected signal, measuring the interval time and then the distance between the instrument and the scanned surface. Alternatively, an optical laser imager projects planes of laser light onto a mold while digital cameras record the shape of the curve of light as it hits the surface. Reconstruction algorithms are used to establish the mold or cast shape[4, 9, 13]. The scanning technology and accuracy had been previously assessed [14]. The technique is noninvasive and produces a detailed 3D model of the face. During the digitization process, the subject is required to remain still while the scanner acquires the details of the subject's head.

A portable hand-held laser scanner (FastSCAN Cobra; Polhemus Inc, Colchester VT) is an example for data collection; actual anthropometric calculations were performed off-line. The reported precision of the laser scanning device is approximately 0.5 mm, and time of exposure from ear to ear, trichion to menton scan, is 20-30 seconds (Figure 5a) [15, 16]. Furthermore, following the same principles, table scanners (Figure 5b) are used to digitize inanimate objects.

- *Photogrammetry*

Photogrammetry is an alternative process of measurement using instruments such as rulers or calipers, obtaining measurements by means of photographs, in practice, determining the geometric properties of objects from photographic images. Generally photogrammetry refers to measurement from 2D photographs, but when researchers have transferred their techniques to medical applications, the term is often used to refer to 3D reconstruction from 2D images and their usage of the term has persisted. In this thesis, the term was used to indicate the derivation of 3D information of objects from their 2D images,

- *Stereophotogrammetry*

Currently, the most promising method of 3D surface imaging system is based on digital stereophotogrammetric technology. These systems are capable of accurately reproducing the surface geometry of the face, and map realistic color and texture data onto the geometric shape result in a lifelike rendering (Figure 6).

This method typically consists in a group of cameras with a fast capture time; the cameras capture different images of the subject from multiple angles simultaneously (Figure 7), and dedicated software reconstructs a digital 3D image. These systems offer a number of distinct

advantages: minimal invasiveness, quick capture speeds (often under one second), and the ability to archive images for subsequent analyses. A quick image acquisition reduces the effect of subject movements; also, there is no need for direct contact with the facial surface, thereby avoiding modification of soft tissues, which may cause errors in direct measurements[3, 17-19].

In this thesis, the stereophotogrammetry system used was Vectra 3D Imaging System (Canfield Scientific, Inc., Fairfield, NJ, USA), which consist in a modular 3D image capturing system designed to capture and process stereo images. The system consists of 2 pods, including 3 cameras (2 black-and-white and 1 color) and a projector in each pod. Basically, the method of active stereophotogrammetry is used: a fine pattern is projected onto the facial surface, thus magnifying the differences between facial areas of various depth. Subsequently, synchronized 2-dimensional images of the subjects are captured within 0.75 ms. By use of dedicated software, the information is used to work out the 3D reconstructions that subsequently can be processed, analyzed, manipulated, and measured (Figure 7). A calibration step is required daily and before patient arrival or anytime the system has been moved.

1.1c Statistical Methods errors

Technical error of measurement (TEM)

Auxiliary precision estimate was included in this study to evaluate the random error: Technical error of measurement (TEM) or Dahlberg's error. Also called the method error statistic or Dahlberg's errors, this is one of the most widely used test for precision[3, 20, 21]. When using two measurements, TEM is computed as:

$$TEM=\sqrt{\sum D^2}/2n$$

Where "D" represents the difference between the repeated measures and "n" represents the number of analyzed individuals.

Mean Absolute Difference (MAD)

MAD is expressed as the average of absolute differences between the values of two sets of measurements[3, 19]. The MAD was commonly reported as a precision estimate[3, 19]; it has a simple calculation and easy interpretation. MAD is computed as:

$$MAD = \Sigma \left| D \right| / n$$

Where "D" represents the difference between the repeated measures and "n" represents the number of analyzed individuals.

Relative Error Magnitude (REM)

REM represents an estimate of error magnitude relative to the size of the measurement, expressed as a percentage. The REM was obtained by dividing the MAD for a given variable by the grand mean for that variable and multiplying the result by 100; it represents an estimate of error magnitude relative to the size of the measurement. Thus, smaller percentages correspond to more precise measurements. According to Weinberg et al.[3], REM scores were divided into five precision categories: values less than 1% were considered "excellent," from 1% to 3.9% - "very good," from 4% to 6.9% - "good," from 7% to 9.9% - "moderate," and exceeding 10% were considered "poor."

Accuracy errors

Accuracy errors (AE, unit: %) were used to compare the measurements with the reference values. This index represents an estimate of error magnitude relative to the size of the measurement. Thus, smaller percentages correspond to more precise measurements.

$$AE = \frac{\text{Real value} - \text{measured value}}{\text{Real value}} \times 100$$

Systematic Errors

Paired Student's t tests were used to compare the systematic errors between the replicate measurements. A p value of 0.05 or less was used to assess statistical significance.

1.2 Aim

In our laboratory we have been working with 3D facial measurements since the late 80's. Both contact and optical instruments have been used for data acquisition, focusing on the 3D position of soft tissue landmarks[22-29].The various instruments have several advantages and limitations[4, 30]

This thesis will present the most recent investigations to assess landmark localization from 3D stereophotogrammetry, concentrating on those methods that have used image processing algorithms to provide a degree of automation.

2. Study 1- A photographic system for the three-dimensional study of facial morphology

Three-dimensional reconstruction has great potentialities for diagnosis of patients' abnormalities or syndrome delineation, having the potential to compensate the inadequacies of a 2D image, so improving the multi-disciplinary and multi-species studies of genotype–phenotype correlations through simple and precise measurements[31-34]

Current devices for facial 3D analysis are costly, impeding their routine clinical use. Additionally, they often need dedicated spaces, which cannot be organized within dental and orthodontic offices, thus limiting the use of 3D analysis to university laboratories and research centers. As the use of digital photography and computer imaging increases, morphometric evaluation must become a simple and cost-effective method to assess soft tissue changes in a reliable way.

The aim of this study was to test whether digital facial photographs supported by a commercial 3D software program are suitable for measuring the soft tissues of healthy subjects when compared with data obtained by a certified 3D computerized electromagnetic digitizer.

2.1 MATERIALS AND METHODS

Fifteen healthy volunteers were included in this study, 11 men and four women, ranging in age from 22 to 28 years. None of the volunteers had undergone previous operations, had a history of craniofacial trauma or congenital anomalies. All procedures were non-invasive and carried out with minimal disturbance to the subjects. The study was performed in accordance with the Declaration of Helsinki, with institutional ethics committee approval, and all subjects provided written informed consent. Their facial characteristics were described by the set of 50 soft-tissue landmarks currently used in the laboratory (section 1.1a)

The majority of the 50 soft tissue facial landmarks were previously identified on the subject face with black liquid eye-liner, except for the inferior and superior point of the nostril axis (Itn; Stn), exocanthion (Ex), endocanthion (En), stomion (Sto) and cheilion (Ch).

After facial landmark identification, their coordinates were collected with two different methods: a 3D computerized electromagnetic digitizer and photogrammetry (Photomodeler).

3D computerized electromagnetic digitizer (Polhemus)

Three-dimensional (*x*, *y*, *z*) coordinates of the facial landmarks were obtained with a 3D computerized electromagnetic digitizer (3Draw, Polhemus, Colchester, VT). Using the instrument stylus, a single operator digitized the marked landmarks while the subjects sat motionless with a natural head position.

Using a computer program, the files of the 3D coordinates obtained were used for all the subsequent off-line calculations, based on Euclidean geometry. With the geometric models of the face (Figure 8) defined by Ferrario *et al.*[5, 8], the x, y, z coordinates of the landmarks obtained for each subject were used to calculate a set of facial angles and distances, as described in table 1. A detailed description of the procedure can be found in Ferrario *et al.*[5]

Photogrammetry surface imaging system (PhotoModeler)

To assess whether the measurements provided by the photogrammetry surface imaging system were comparable to the electromagnetic digitizer, the same distances and angles were computed for both methods.

Three single photographic images (Figure 9) from different angles were taken using a tripod to steady the camera. Assisted by specific software (PhotoModeler Pro, EOS Systems Inc), the landmarks were assigned and referenced in each picture. Subsequently, geometric models of the face of each subject were obtained and distances and angles calculated (Figure 10).

The subjects' pictures were taken using a 6.0-mega pixels digital camera (Sony DSC – H2 Cybershot, Sony Corporation, Japan). Reference paper marks were placed on the wall behind the subjects to provide a subsequent metric calibration (Figure 11).

Error of method

To verify the reproducibility of the tracings of the photographs, measurements from three random subjects were re-performed at interval of 1 month to further reduce the potential for memory bias.

In addition, to analyze a further possible error (reproducibility during rearrangement), new three subjects were included in two different photographic sessions. In this time, the camera and the subject's position were modified between each photo and between the replicate sets.

Statistical Analysis

An auxiliary precision estimate was included in this study to evaluate the random error. Allied with the descriptive statistics (mean and standard deviation), the mean absolute difference (MAD) from the values of electromagnetic digitizer and Photomodeler across each subject was calculated for all the linear distances and angles (section 1.1c).

Data obtained with the two imaging systems were compared using paired Student's *t*-tests. For all analyses, a *P*-value of 0.05 or smaller was considered significant.

2.2 RESULTS

Tables 2 and 3 report the descriptive statistics for linear distances and angles computed in the analyzed subjects.

Among the 12 considered linear distances, two mean differences between measurements obtained via electromagnetic digitizer and photomodeler were significant. The mean absolute differences (MAD) across the measures were typically less than 1.62 mm, except two linear measures, which were the medium width of the face (T*r*-T*l)* and the inferior depth of the face (Pg-T). (Table 2)

Three of the 18 analyzed angles also showed a statistically significant difference between the two techniques, revealing a discrepancy in the facial convexity (Tr-N-Tl), (Tr-PrN-Tl) and (Tr-Pg-Tl). Nevertheless, in these variables the difference between the means was smaller than 1.81 degrees, contrasting with the angle Ex*r*-N-Ex*l,* which presented a MAD of 2.51 degrees (Table 3).

The technical errors of measurement (TEM) were used in repeated digitizations of the photographs to analyze the random error. Lower TEM values correspond to more repeatable measurements. The highest values were observed for the exocanthion (Ex) in both distance and angle analysis, followed by the gonion (Go) in angle evaluation (Table 4). In no occasions, systematic errors were found (all t-tests were not significant).

When the subjects and the camera were moved among each set, all error values were increased (Table 5), showing the highest values of 5.26 mm for tragus (T) for linear measurements and 5.61º for the landmarks involving the labial area in the angular measurements. However, no systematic significant differences were found between the replicate measurements ($p>0.05$) (Tables 4 and 5).

2.3 DISCUSSION

When describing growth patterns or anatomical variations, 3D imaging systems are growing on the usage of craniofacial morphometry with great clinical applications in diagnosis, presurgical planning, postsurgical outcomes and syndrome identification.

A number of relatively noninvasive methods for 3D imaging have been developed over the last decades to obtain anthropometric data from the face[3, 4, 31].

The system used in the current study permits the indirect digitization of single facial landmarks using the same criteria of the electromagnetic digitizer[5, 8]. This research includes the development of a simple, low cost and non-invasive three-dimensional method for facial surface measurements. It eliminates the need for direct contact with the subject, thereby avoiding displacement/deformation of soft tissues[19]. The co-ordinates of the landmarks can be used for off-line calculation of distances and angles. Any new measurement can be evaluated from the same landmarks without any new data collection.

Comparing this three-dimensional photographic system (Photomodeler) and the electromagnetic digitizer will add some advantages and limitations. In both methods, the facial landmarks may be identified and marked on the face of each subject by a single experienced investigator. Unlimited number of landmarks should be identified only once, independent of the number of subsequent measurements, thus reducing method error.

The photomodeler system needs a picture set as reference to make the triangulation: generally frontal pictures were used as reference. Consequently, the main problem of this system seems to be marker location, where some landmarks cannot be assigned in the reference pictures. One of the indistinguishable landmarks often happened to be Tragus (T). This may explain the results obtained in this study, which showed differences in two linear measures (T*r*-T*l*; Pg-T) and also in three angles (T*r*-N-T*l*; T*r*-PrN-T*l*; T*r*-Pg-T*l*); all of these variables involve Tragus.

The mean absolute difference (MAD) was commonly reported as a precision estimate[18, 19], it has an easy interpretation and it is of simple calculation. In the current study, the highest variations were found in distances including the Tragus and Gonion landmarks, and in angles of facial convexity on the horizontal plane, that crossed both facial halves. This result is in accord with Weinberg *et al.* [3], and it can be explained by the difficulty of assigning the lateral landmarks in reference photos. For the 'Ex' landmarks, two factors should be considered: in some cases, the non-correct identification caused by the eyelash; in other cases, the lack of a previous identification with a black mark.

Furthermore, the presence of hairs may mask some landmarks, resulting in some missed landmarks or the non-identification of some points in all the three photos. In this case, after analyzing and processing all evident landmarks, the software gave us an approximated location of the missed landmark locations in all pictures to complete the geometric 3D reconstruction. Thus, good pictures with fine resolution are required to minimize errors.

The reproducibility of the 3D computerized electromagnetic digitizer throughout landmarks identification and marker positioning was previously reported[5, 8]. According to the anthropometric literature[18, 24, 35], the technical error of measurement was included in this study to verify the reproducibility of the Photomodeler system. The highest method error for linear measures (distances) between the first and second sets of Photos was 1.57 mm for the exocanthion, without significant systematic difference. Therefore, the results indicate acceptable repeatability in two different occasions.

Similarly, differences of more than 2° were observed in four angles (Ex*r*-N-Ex*l*; Go*r*-Pg-Go*l*, Li-Sl-Pg; (SN-Ls)-(Li-Pg). Although just 3 subjects were used for this error examination, the outcome agree with Weinberg *et al*. [3], who reported that the estimation of error magnitude tended to be higher in variables containing difficult-to-see landmarks and variables crossing the labial fissure.

For the photomodeler system, the photographs are taken in different moments and angles and a possible movement of the head may occur, hence its influence on data collection during subject and camera relocation was evaluated. As a result, increased values in errors of reproducibility were observed. In this manner, the subjects should be advised to not make great movements during the photo acquisition.

In summary, these results showed that the system is capable of measuring the same object by a satisfactory degree of repeatability, but some landmarks need to be re-evaluated, improving the acquisition. Hence, the technique could provide an easy and useful way for understanding the information and establish a diagnostic or therapeutic method.

2.4 CONCLUSION

The three-dimensional photogrammetry system tested in the present study can assess the coordinates of facial landmarks with satisfactory precision, and reliable facial measurements can be obtained. The method is relatively fast, and non-expensive equipment is needed, being simply to be used for private clinics, researchers or practitioners. These analyzes established that photomodeler system measurements can be used for linear distances and angles. However, more studies should be performed to improve the protocol, enhancing its accuracy.

3. Study 2 - Accuracy and reproducibility of a 3d stereophotogrammetric imaging system

Several systems using three-dimensional stereophotogrammetry have been described in the literature[3, 17, 19, 34, 36-38]. However, some methods found problems of reproducibility of specific soft-tissue landmarks which localization depended on the underlying skeleton, such as gonion and zygion[39].

Independently of the technique used for taking three-dimensional measurements of facial soft tissues, accuracy and validity of the method are fundamental for a reliable analysis of craniofacial deformities[3, 18, 19, 31, 34, 36, 38, 40-43].

The aim of this study was to assess the accuracy and reproducibility of a 3D stereophotogrammetric imaging system (Vectra-3D, Canfield Scientific, Inc., Fairfield, NJ, USA) on measuring the facial soft tissues of healthy subjects. A quantitative analysis of the possible errors was made.

3.1 MATERIALS AND METHODS

Experimental design

Data from a standard geometric objects and from 10 healthy individuals without a previous history of craniofacial trauma or with congenital anomalies were collected to verify accuracy and possible errors during stereophotogrammetric acquisitions and calculations. For all acquisitions, a commercial 3D stereophotogrammetry system was used (Vectra 3D)[17, 38].

Accuracy on Standard Objects

To assess the accuracy of the 3D stereophotogrammetry instrument, a set of measurements were made using standard objects (cubes and cylinders of different dimensions). Images of the geometric objects were taken with a measuring grid with a 1 mm of resolution (Figure 12), and measurements were performed for linear distances (unit: mm), angles (unit: degrees) and areas (unit: cm^2). Data were saved and analyzed using the Vectra's image processing software.

Facial Measurements

Ten healthy volunteers were included in this study, 5 men and 5 women, ranging in age from 20 to 30 years. No selections on specific facial characteristics were made.

All procedures were noninvasive and were carried out in accordance with the Declaration of Helsinki, with institutional ethics committee approval and with minimal disturbance to the subjects, who were previously informed about the adopted procedures, giving their consent to the investigation. Sample size was determined considering a mean difference between repeated acquisitions of 1 mm (SD, 1), with an error set at 0.05 and an error set at 0.8.

By use of a black liquid eyeliner, the 50 soft tissue landmarks were marked, except for the inferior and superior point of the nostril axis (Itn and Stn), exocanthion (Ex), endocanthion (En), stomion (Sto), and cheilion (Ch). The reproducibility of landmark identification and marker positioning has previously been reported and found to be reliable.

After facial landmark marking, their coordinates were collected by use of the 3D stereophotogrammetry imaging system (Figure 7). The 3D images obtained from the subjects were analyzed, and a set of facial distances among the landmarks were calculated (Table 6).

- Calibration error

Considering that the equipment must be calibrated before daily work, or after any change of the apparatus, like tripod displacement, possible calibrations errors were assessed. Two sets of acquisitions (1st and 2nd) were performed for each subject; the machine calibration was re-done before each set of acquisitions. The distances calculated from the first and the second set, were compared.

- Inter-operator digitization error

To investigate the reproducibility between different operators' tracings, the same landmarks were assigned and referenced by two separated operators (1st and 2nd operator).

- Two sets acquisition error/digitalization

To analyze the reproducibility after subject re-positioning, the subjects were included in two different photographic sessions (1st and 2nd acquisition): subject's position was modified between each acquisition.

Statistical Analysis

For the assessment of system accuracy, means and standard deviations were computed for distances, angles and areas calculated on the standard geometric objects; paired Student's t tests were used to compare the measurements with the reference values.

For all facial measurements, together with the descriptive statistics (mean and standard deviation), the Mean Absolute Difference (MAD) across each data set was calculated (section 1.1c).
Paired Student's t tests were used to compare the systematic error between the replicate measurements. A p value of 0.05 or less was used to assess statistical significance. The technical error of measurement (TEM) was used to evaluate the random error (section 1.1c).

3.2 RESULTS

Table 7 reports the measurements obtained on the standard objects for linear distances, angles and areas. The differences between measurements obtained on the geometric objects were quite low, and were nearly similar to the resolution of the grid. All measurements obtained on the cubic box were very accurate: the distance was 10.02 mm (SD, 0.03); the mean angle, 89.96° (SD, 0.19); and the mean area, 1.00 cm^2 (SD, 0.01). Somewhat larger errors were obtained on the cylindrical objects, with errors up to 1.21%.

All values were not significantly different from the actual values (P>0.05, paired Student t test).

No systematic errors between measurements obtained with 2 different calibrations were found (Table 8, all P values from paired Student t tests were larger than 0.05). All mean differences were lower than 0.25 mm, with MADs ranging between 0.13 mm (nasion-subnasale distance) and 1.19 mm (mouth width). Accordingly, the lowest TEM was found for N-Sn distance and the largest for mouth width. Lower TEM values correspond to more repeatable measurements: the random error was lower than 0.5 mm in 10 of 16 distances, it was between 0.5 and 1 mm in 5 distances, and it was larger than 1 mm only in 1 distance.

Data obtained by 2 different operators all had negligible random errors (Table 9), with MAD values ranging between 0.05 mm (inter-zygia distance) and 0.9 mm (mouth width). No systematic errors were found (P>.05), and all TEMs were lower than 0.7 mm.

When the same subjects were measured twice with the same calibration (Table 10), the MADs across the measures were typically less than 1.0 mm, except for mouth width, whose MAD was 1.18 mm. The largest TEMs (random errors) were found for mouth width and lower anterior facial height (0.91 mm), followed by N-Pg distance (0.86 mm). No systematic errors were found for the analyzed distances; in 12 of 16 distances, the first acquisition yielded a larger value than the second one.

Overall, the analyzed subjects had different facial forms, and both hypo- and hyper-divergent faces (posterior–to–lower anterior facial height ratios ranging between 89% and 136%), dolichocephalic and brachiocephalic faces (facial height–to–facial width ratios ranging between 75% and 92%), and occlusal and skeletal Class II and Class III facial patterns (midfacial depth–to–mandibular corpus length ratios ranging between 127% and 157%; upper lip to pronasale-pogonion line distance ranging between 3.2 and 9.3 mm; lower lip to pronasale-pogonion line distance ranging between 1.3 and 7.9 mm) were measured. A slight mandibular asymmetry (deviation from midline up to 6 mm) was also observed in 3 subjects. On no occasion was there a relationship between a specific facial form and measurement errors.

3.3 DISCUSSION

Several techniques such as ultrasound, laser scanning, computed tomography, magnetic resonance imaging, and electromagnetic digitization can analyze facial characteristics in 3 dimensions, but stereophotogrammetric systems are becoming the instrument of choice in anthropometric investigations[17, 44].

The advantages of stereophotogrammetric systems include the lack of contact of the instruments with the cutaneous surface during measurement and the shorter period of interaction with the patient, because features are measured after data acquisition. Thus any new measurement can be obtained from the digital database without any new data acquisition. In addition, digital anthropometry was shown to be as precise as (or even better than) direct measurements[3, 18, 31, 45, 46].

The current study showed that the Vectra 3D Imaging System was both accurate and repeatable. Measurements on the standard objects showed good accuracy; the obtained values were close to the real values, ranging from 0.04% to 1.21%, and with a mean accuracy error of 0.50%. Actually, the minimal differences found could be associated to the operator digitization or the printed grid used.

The assessment of system accuracy is obviously necessary before implementing its clinical use as a measurement tool.

To assess the reproducibility of the system for clinical measurements, a set of linear distances was selected among those most used for the quantitative analysis of facial characteristics[29, 42].

The distances covered all facial surfaces and were made in all 3 spatial planes: horizontal—Ex-Ex, T-T, Zy-Zy, Go-Go, and Ch-Ch; vertical—Tr-N, N-Sn, Sn-Pg, N-Pg, and T-Go; and anteroposterior—N-T, Sn-T, Pg-T, Pg-Go, Ls–(Prn-Pg), and Li–(Prn-Pg)[3].

In addition, distances with mean values ranging from 4 (lower lip to Prn-Pg line) to 140 mm (inter-zygia distance) were selected to assess the quality of measurements over all ranges of clinical interest. Subjects were not selected for a specific facial pattern, and they had different facial forms in all 3 spatial planes.

Before stereophotogrammetric acquisition, almost all landmarks were marked on the facial surface, as described by Ferrario et al.[5] Indeed, previous investigations found that marked landmarks were associated with smaller errors than unmarked ones. This procedure allowed the assessment even of the bone related soft tissue landmarks, which were neglected in previous studies[3, 39] or substituted by similar landmarks with different definitions[46].

The system was reliable in the assessment of most of the studied linear distances. No systematic errors were found; on average, the actual differences between repeated measurements were lower than 1 mm. Overall, measurement errors were not related to the different facial morphologies.

Analyzing the errors resulting from the calibration procedure, we found that the MAD values showed the lowest accuracy for mouth width, with a difference of 1.19 mm between the repeated measurements. In fact, because the corresponding landmarks had not undergone previous identification with the black liquid eyeliner, this little difference may come from the landmark digitization[31] instead of from a calibration inaccuracy. Similarly, when analyzing the inter-operator errors and the repeated acquisitions, we again found the largest MADs for the Chr-Chl distance. Therefore it is recommended to mark all the considered landmarks before any stereophotogrammetric acquisition[3, 19].

On the basis of the digitization error between 2 different acquisitions, almost all measurements were very reproducible. For instance, all the linear distances had TEM values lower than 1 mm. The largest reproducibility was found for the distance between the 2 zygion landmarks, with a TEM of 0.09 mm. However, the distances Chr-Chl, Sn-Pg, and N-Pg showed somewhat larger errors. Together with the lack of previous landmark identification with a black mark for Ch, some disparities could be explained by facial hairs: the presence of a beard in some male subjects

may mask the landmark Pg. Both Wong et al.[19] and Majid et al.[37] found that the presence of hairs may cover some landmarks, resulting in some missed values or in increased errors. Mouth measurements also had the largest errors in the investigation of Ghoddousi et al.[31]

The linear distances Zy-Zy, T-T, N-T, Ls–(Prn-Pg), Li–(Prn-Pg), and N-Sn had also quite low error values in all tests, with MAD values lower than 0.3 mm. Between different operators, smaller errors tended to be associated with landmarks on the middle line (vertical distances), independently from slight facial asymmetries. The outcome diverges with that of Weinberg et al,[3] who reported that the estimation of error magnitude tended to be higher in vertical distances crossing the labial fissure, but it is in good accord with that of Plooij et al.[46]

In contrast with previous studies that reported that stereophotogrammetric and laser scanning instruments had difficulties in digitizing the tragion (T),[3, 34, 41, 46] we could assess this landmark with good reproducibility. All the relevant distances (horizontal, T-T; vertical, T-Go; and anteroposterior, N-T, Sn-T, and Pg-T) had MAD and TEM values lower than 0.5 mm for repeated acquisitions (except Pg-T) and lower than 0.4 mm for between-operator and calibration errors (except Pg-T). The possible masking effect of facial hairs on the chin has already been discussed.

Different facial morphologies, with variations in ear position and dimensions, may explain the contrasting results for tragion landmark found in literature. In addition, to reduce the masking effect of facial hairs, when necessary, we wet the region just anterior to the earlobe and try to put all hairs behind the earlobe. Nevertheless, the ears still remain a part of the face where digitization is difficult, notwithstanding their importance for facial anthropometric and clinical descriptions[4, 47].

3.4 CONCLUSION

In conclusion, this study found the used stereophotogrammetric system both accurate and repeatable; error magnitude scores derived from the imaging system showed a high degree of precision, comparable to previous reports performed not only on living subjects[19] but also on mannequins and facial casts[18, 34, 36].

Several facial types were assessed, and errors were not dependent on specific facial morphologies. The method could therefore be useful for clinical analysis in maxillofacial, plastic, and esthetic surgery, as well as in all dental fields, where modifications of the soft tissues are made. Further investigations should assess system errors in subjects in other age ranges, as well as in patients with severe facial disfigurements[17, 29, 41, 42, 48].

4. Study 3- Digital dental cast placement in 3-dimensional, full-face reconstruction: A technical evaluation

Alongside whole with the recent development of 3D digitizers for facial surface, current technology also allows to digitize in the 3D space the dental models, and the association between the digital dental cast and the 3D facial images could allow the clinician to analyze the relationship between soft tissues and dental arches, avoiding when possible the use of X rays [49].

Rangel et al. [49] proposed the integration of a digital dental cast into a 3D facial picture. According to the average distance between the matched areas (anterior teeth) in one patient, the method was reported to be reliable, but larger studies are necessary to verify if a matching between the digital dental cast and the 3D facial image could correspond to the correct position of the whole dental arches.

As the matching between the 3D face and the digital dental casts done by stereophotogrammetric systems must use the anterior teeth as reference, any displacement or inclination of the digital dental arch would add a position error in the posterior dental region. Therefore, the aim of this study was to elaborate and validate the matching between digital dental casts and stereophotogrammetric images as a non-invasive 3D reconstruction of dento-facial structures in healthy subjects, analyzing distances between the occlusal plane and facial landmarks.

4.1 MATERIALS AND METHODS

Experimental design

Healthy subjects were selected to have their maxillary dental casts digitized by laser scanning and their 3D facial soft tissues acquisition merged in a single file. Seven linear distances through facial and dental landmark were measured and compared between in vivo and virtual reproductions to quantify the accuracy of the final 3D reconstruction.

Subjects

A group of 11 healthy volunteers, 4 men and 7 women, ranging in age from 20 to 31 years, without a previous history of craniofacial trauma or with congenital anomalies and with full maxillary and mandibular dental arches were selected. All procedures were noninvasive and were carried

out with minimal disturbance to the subjects, who were previously informed about the adopted procedures giving their written consent to the investigation, following the principles outlined in the Declaration of Helsinki.

Digital Dental Casts

For each subject, a maxillary dental reproduction was obtained by an irreversible hydrocolloid (Tropicalgin, Zhermack SpA, Badia Polesine, RO, Italy) and cast with a type 3 model dental stone (Elite Model, Zhermack SpA, Badia Polesine, RO, Italy). Using a commercial laser scanner (D100, Imetric 3D GmbH, Courgenay, Switzerland- Figure 5b), dental casts were digitized and the appropriate files imported into the stereophotogrammetric software.

Virtual facial reproduction

Soft tissues facial morphology was acquired by a 3D stereophotogrammetry imaging system (Vectra-3D; Canfield Scientific, Inc., Fairfield, NJ, USA). The reproducibility of stereophotogrammetric technology was well documented [3, 19, 34, 36, 40, 50, 51]. In particular, method error was tested in the Study 2 of the current thesis, finding stereophotogrammetric system both accurate and repeatable.

Before each acquisition, three soft-tissue landmarks (N: Nasion; Ftr: frontotemporale right, Ftl: frontotemporale left) were marked on the face with black liquid eye liner [8] for further analysis. For each subject, two sets of facial 3D images were obtained: one with open lips (with cheek retractors) with visible frontal teeth, and another one with the teeth in occlusion and closed lips (Figure 13).

Matching

To obtain virtual dento-facial reproductions, the matching between the 3D facial images and the corresponding maxillary digital dental arch was made using Vectra's software tools. The matching process followed three steps (Figure 14):

A. The digital dental cast was merged with the open lips facial acquisition
B. The image with closed lips was introduced into the scene to be related to the open lips image

C. The open lips acquisition was removed from the file, obtaining a final digital image with the dental cast and the facial reconstruction with closed lips in the relevant 3D positions (See Video, Supplemental Digital Content 1, which demonstrates the final digital three-dimensional reconstruction).

Reliability and accuracy

- Virtual teeth positioning accuracy

To verify the accuracy of the "virtual" full reproduction, the 3D coordinates of the three facial (nasion, right and left frontotemporale) and of three dental (I: inter-incisor; Pr, Pl: tip of the vestibular cuspids of right and left first permanent premolar) landmarks were obtained directly on each subject (in vivo) using a 3D computerized electromagnetic digitizer (Polhemus – section 1.1b) Seven linear measurements were then mathematically computed from the 3D coordinates, and calculated using Euclidean geometry (Table 11).

The same linear distances were also obtained from the 3D digital reproduction using Vectra's software tools (Figure 15).

- Matching reliability

To investigate the reliability of matching between the images, the merging procedures described above were done twice (1st and 2nd matching) and the distances reported in Table 11 were calculated on each matching.

- Matching accuracy

As the merged images were done using two different photos (closed and open lips, Figure 14B), to assess the accuracy of Vectra's matching, a random area in the forehead was selected for each "closed lips" photograph, and the distance from the respective "open lips" pictures was evaluated. Ideally, this part of the face should not move with open lips.

Statistical analysis

Paired Student's T tests were made between the distances computed in vivo and on the virtual reproduction to detect possible systematic errors. P values smaller than 0.05 were considered significant.

Mean absolute difference (MAD), technical error of measurement (TEM) and relative error magnitude (REM) were calculated to quantify the precision of the adopted protocol (section 1.1c).

4.2 RESULTS

The mean and standard deviation of virtual and in-vivo measurements are reported in Table 12. Statistically significant differences were detected in three distances (N-I, Ftl-Pr and Ftl-I), with p values from the paired Student's t tests lower than 0.05. In all occasions, the mean absolute differences were equal or lower than 1.2 mm.

The technical error of measurement ranged between 0.6 and 1 mm. The relative error magnitude (an estimate of error magnitude relative to the size of the measurement) ranged between 0.9 and 1.2%.

Table 13 reports statistical analysis of reliability of matching procedures. No significant differences were found between repeated merging. MADs and TEMs values resulted lower than 0.6 mm.

The mean distance between the foreheads (face with open lips vs. face with closed lips) was 0.4 mm, ranging between 0.04 and 1.1 mm (Table 14).

4.3 DISCUSSION

Many dysmorphic syndromes or craniofacial anomalies that involve dental-facial relationships can potentially be analyzed by a combination of soft- and hard-tissue assessments [41, 44, 49, 52]. In several clinical applications, virtual reproductions of human morphology can aid the practitioners during diagnosis and planning of medical procedures and treatments.

Currently, x-ray technology allows reproducing both the three-dimensional morphology of teeth and of soft-tissue facial structures[44], but in a quite invasive way throughout radiation. Indeed, clinicians should attentively consider the risk-benefit to the patient also when obtaining craniofacial

images, and current research is trying to reduce unnecessary radiographic exposures, especially in children[49, 52, 53].

In the current study a non-invasive protocol to reproduce dento-facial features was defined and evaluated. The two virtual facial reconstructions were very well matched each other, with mean errors of 0.4 mm, a value in perfect accord with that reported by Rangel et al. [49] for a single patient matching. Indeed, the reliability tests demonstrated a good quality 3D image managing with TEMs and MADs lower than 0.6 mm and no systematic errors. Also, the results showed a satisfactory agreement between virtual reproductions and in-vivo acquisitions. Despite three distances (N-I, Ftl-Pr and Ftl-I) showed statistically significant differences, the TEMs and MADs were always lower than 1.0 mm and 1.2 mm respectively, with REM (relative error) up to 1.2%. Overall, these errors are within an acceptable range for clinical and anthropometric contexts[54, 55]. Such findings could be explained by software precision. Indeed, the high quality surface texture is helpful to recognize the landmarks, increasing matching precision.

The main technical complication was due to tooth translucence allied with saliva biofilm that often resulted in unsatisfactory virtual tooth reconstructions. Maintaining tooth surface dried was an important step to obtain satisfactory results. Overall, the protocol defined in the current investigation resulted appropriate to the initial purpose.

Further studies are necessary to improve the protocol, finding a reliable way to associate the virtual mandibular dental arch with the 3D digital facial reconstructions, thus allowing the daily use of the protocol, mostly within research facilities. Indeed, another limit of the described protocol may be the cost of the technical instruments for the private dental office.

4.4 CONCLUSION

In conclusion, merging digitized dental maxillary arch and 3D stereophotogrammetric facial acquisition could provide a reliable reproduction of dentofacial relationships. The method could be used to monitor longitudinally the evolution of orthodontic/ orthopaedic healing through a non-invasive acquisition of dental and facial morphology, thus guiding the clinicians in a “real time” management of the treatment. The reduction in X-ray exposure and the use of a global three-dimensional analysis are probably the main benefits of the method.

5. Study 4 - Unilateral cleft lip and palate (UCLP): a 3D evaluation

Cleft lip/ palate (CLP) represents the most frequent congenital malformation of the head and neck. Often occurs in isolation with an incidence of approximately 1/ 700, varying with the specific type of cleft, geographic location, ethnic group and socio-economic conditions and in association with other malformations has been long recognized, with a reported frequency between 3% and 63% [56]. Although the treatment of children with CLP has improved over the years, deficient growth of the maxilla is still common. The reasons of abnormal facial morphology in treated cleft individuals may involve two factors: intrinsic developmental deficiency or iatrogenic factors introduced by treatment[57].

The palate, and its three-dimensional (3D) reproductions with stone casts, are complex structures, that cannot be easily analyzed with conventional two-dimensional methods (photographs, radiographs) [58, 59]. The problem is particularly important for CLP patients, where the quantitative assessment of the depth of the cleft can be better done with 3D imaging methods [59-62].

Currently, palatal models of patients can be scanned by laser to obtain 3D virtual models that can be used to perform measurements needed for treatment planning [60]. Additionally, virtual models allow an easier communication between clinical areas and specialties due to the facility in sharing files. Biological structures can be scanned also by other optical instruments, like stereophotogrammetry, a method that is currently most used for the imaging of soft tissues[23, 27], but that may be efficaciously employed also for stone casts [63].

Although 3D virtual palatal models may be an advantageous tool in CLP patient analysis and planning, a necessary prerequisite is that measurements performed on these 3D virtual models are reliable and valid. Therefore, this study has the aim to assess a 3D stereophotogrammetric method for palatal cast digitization of children with UCLP. Data obtained with the 3D method will also be compared to conventional caliper measurements.

5.1 MATERIALS AND METHODS

Experimental design

Ninety-six palatal cast models obtained from neonatal patients with unilateral cleft lip and palate (UCLP) attending the Fundación Clínica Noel de Medellín (Colombia) were analyzed. Palatal casts were collected during a clinical study performed to evaluate the 3D morphological effects of various treatments on the growing segments of dental arches of patients with UCLP.

Anatomical references (landmarks) on cleft dental casts

Before the digitization, landmarks were marked on each palatal cast. The anatomical reference landmarks assessed the two cleft segments separately (Table 15, Figure 16).

Dental Casts Digitization

Using a commercial 3D stereophotogrammetry system (VECTRA-3D, Canfield Scientific, Inc., Fairfield, NJ, USA), the palatal casts were digitized and the appropriate files were analyzed using the stereophotogrammetric software [23]. The 3D coordinates of the selected landmarks were obtained.

Digital dental cast measurements

Using the landmark coordinates, anterior-posterior, transverse and vertical linear distances were obtained as described in Table 16. All the measurements were made with the "point-to-point" distance tool of the stereophotogrammetric software.

Digitization error

To investigate the reproducibility between the operators' tracings, the same landmarks were assigned and referenced twice by the same operator (A1 and A2).

Caliper measurements

Starting from the same landmarks described above, the same linear distances were measured on the palatal casts using a caliper with a 0.05 mm precision. The obtained values were compared with the 3D measures provided by the stereophotogrammetric system.

Statistical Analysis

For the assessment of system accuracy, means and standard deviations were computed for distances, angles and areas calculated on the standard objects. Accuracy errors were used to compare the measurements with the reference values (section 1.1c)

For palatal cast measurements, together with the descriptive statistics (mean and standard deviation), the Mean Absolute Difference (MAD) across each data set was calculated. (section 1.1c) Paired Student's t tests were used to compare the systematic errors between the replicate measurements. A p value of 0.05 or less was used to assess statistical significance.

Finally, another accuracy estimator, an error magnitude relative to the size of the measurement (REM), was calculated (section 1.1c). The same calculations (MAD, TEM and REM) and statistical tests (paired Student's t test) were made to compare linear distances obtained by stereophotogrammetry and by caliper.

5.2 RESULTS

No systematic errors between measurements obtained in two different occasions by the same operator (A1-A2) were found (Table 17, all p values from the paired Student's t tests were larger than 0.05).

All mean differences were lower than 0.2 mm, with mean absolute differences ranging between 0.05 mm (Dg-Cg distance) and 0.32 mm (Cg –Cm distance). Accordingly, the lowest TEM was found for Dg-Cg, Ag-Pg and Am-Pm distances, and the largest for Cg -Cm. Lower TEM values correspond to more repeatable measurements: the random error was lower than 0.7 mm for all distances. According to the ranking described by Weinberg et al. (2004), all REM values were considered excellent or with a very good precision.

On Table 18, data obtained by two different methods (caliper vs. stereophotogrammetry) were compared. For all distances, except for Cg –Cm distances, significant systematic errors were found (all p values of paired Student's t tests smaller than 5%), with MAD values ranging between 0.22 and 3.41 mm. Consequently, REM rates were scored "moderate" for Ag –Am and "poor" for Ag-Pg and Am-Pm distance. Indeed, apart from Ag-Pg and Am-Pm distances, all TEMs had small random errors, lower than 1.06 mm. In general, caliper measurements overestimated the analyzed linear distances relative to 3D stereophotogrammetry, except for distances Ag –Am and Ag-Pg (Figure 17).

5.3 DISCUSSION

A variety of methods for facial analyses using 3D reconstructions is offering a significant change in the process of diagnosis, providing information for planning and evaluating medical procedures and treatments[64]. The stereophotogrammetric systems are being spread into the

anthropometric laboratories as good quality instruments for morphologic facial examinations, with several advantages over previous methods such as fast acquisition, limited cost, lack of dangerous procedures, thus becoming the leading tool for surface investigations [3, 19, 23].

At the same time, dental casts can be digitized using laser scanners[65, 66], and the digital models can be used associated with the 3D facial images, allowing the clinician to analyze the relationships between soft tissues and dental arches without submitting the subjects to radiographic scans[27]. Independently of the technique used, the precision and validity of the method are essential for a reliable analysis of craniofacial deformities[3]. The present study showed that a commercial stereophotogrammetric system can be used to digitize the palatal casts of children with UCLP. There are several other anthropometric studies that analyzed palatal cleft deformity using highly sophisticated computerized analytical methods[67, 68], but these methods are not usually available outside the centre that has developed them.

To evaluate the reproducibility of measuring 3D virtual models, a set of linear distances was selected among those most used for the quantitative analysis of UCLP. All reference landmarks were marked on the palatal cast surface previously to stereophotogrammetric imaging. Indeed, previous investigations found that sets with marked landmarks were associated with smaller errors than unmarked ones[3, 19].

The used method was reproducible in measuring the studied linear distances. No systematic errors were found; on average, the differences (MAD) between repeated measurements were lower than 0.32 mm. The mean absolute difference (MAD) and the relative error magnitude (REM) are reported as an accuracy assessment, with a simple calculation and interpretation [3, 19].

Analyzing the errors between the two different systems of acquisition, systematic errors were found for all measures ($p<0.05$), except for Cg–Cm. This could be explained because the landmarks Cg and Cm are located on the crest of the alveolar segments, in an anatomical position that allows an “easy” positioning of the caliper. The differences found between the two measurement methods are in agreement with previous studies which performed linear measurements between reference points with digital calipers directly on the cast models [69, 70]. In both studies, this procedure was found to produce errors not only during the positioning of the landmarks, but also during distance measurement, and when transferring the data into the computer [71]. Indeed, we also observed that the contact of caliper tip on the palatal cast landmark often cancelled the dot, inducing imprecision in the measurements. In a global analysis, caliper seems to overestimate linear distances relative to 3D stereophotogrammetry.

Considering the MAD computed between the two different methods, in most occasions the values were lower than 0.8 mm; hence almost all measurements seemed to have a good accuracy. A different trend was found for the anterior-posterior distances Ag-Pg and Am-Pm that had MADs

of 3.28 and 3.41 mm, respectively. Actually, these same distances, followed by Ag–Am, showed moderate and poor scores, according to the classification used by Weinberg et al [3]. REM analysis was important because it offered an estimated of the relative magnitude of errors, independently from the absolute dimensions[3]. Both anterior-posterior distances showed very large relative errors, which prevent the use of caliper into clinical practice or research. All the other linear distances had TEM values lower than 1.06 mm. The largest reproducibility was found for the distance between Pg -Pm, with a TEM of 0.22 mm. However, the distances Ag-Pg and Am-Pm showed somewhat larger errors. It could be presumed that a largest inaccuracy during the positioning of the caliper tip may be possibly due the point location: Ag and Am are cleft edge points of the alveolar segments, located near to the deformities.

5.4 CONCLUSION

Measurements recorded by the 3D stereophotogrammetric system appear to be sufficiently accurate and reliable for assessing stone casts of newborn patients with unilateral cleft lip and palate. The 3D stereophotogrammetric systems have several advantages over direct anthropometry and gradually are becoming into more accessible cost, replacing classical methods to quantify surface topography. The present study found that the method could therefore be useful for clinical analyses in maxillofacial, plastic and esthetic surgery

6. GENERAL CONCLUSION

Facial soft tissue anthropometry have been used for diagnosing malformations, clinical assessments for surgical procedures (maxillo-facial, plastic, esthetic) or dental treatments (orthodontics, prostheses). Image processing algorithms applied to facial images have the potential to enhance anthropometric applications, reducing time on examinations and improving the reliability of measurements, enabling automatic measurement of clinically relevant distances and angles, as well as shape analysis and comparison[30].

Non-invasive devices for three-dimensional anthropometry offer quantitative and qualitative imaging information about facial soft tissues, improving diagnosis, providing a reliable and fast analysis. Stereophotogrammetry is an efficient method of soft-tissue evaluation that allows trustworthy analysis of craniofacial deformities, supporting fundamental parameters to plan and evaluate maxillo-facial, plastic and esthetic surgery, other than orthodontics and dental treatments. Indeed, stereophotogrammetric system showed to be accurate and reliable for assessing diverse objects, as well as stone casts of newborn patients with unilateral cleft lip. Thus, computerized tools are gradually replacing classical methods to quantify surface topography, facilitating clinical and research studies.

7. REFERENCES

1. Spencer F. History of physical anthropology: an encyclopedia. *Garland Pub*., New York, 1997.
2. Farkas LG. Anthropometry of the head and face. 2nd ed., *Raven Press, New* York, 1994.
3. Weinberg SM, Scott NM, Neiswanger K, Brandon CA, Marazita ML. Digital three-dimensional photogrammetry: evaluation of anthropometric precision and accuracy using a Genex 3D camera system. *Cleft Palate Craniofac J.* Sep 2004;41(5):507-518.
4. Sforza C, Ferrario VF. Soft-tissue facial anthropometry in three dimensions: from anatomical landmarks to digital morphology in research, clinics and forensic anthropology. *J Anthropol Sci.* 2006;84:97-124.
5. Ferrario VF, Sforza C, Poggio CE, Cova M, Tartaglia G. Preliminary evaluation of an electromagnetic three-dimensional digitizer in facial anthropometry. *Cleft Palate Craniofac J.* Jan 1998;35(1):9-15.
6. Ferrario VF, Dellavia C, Zanotti G, Sforza C. Soft tissue facial anthropometry in Down syndrome subjects. *J Craniofac Surg.* May 2004;15(3):528-532.
7. Ferrario VF, Dellavia C, Serrao G, Sforza C. Soft tissue facial angles in Down's syndrome subjects: a three-dimensional non-invasive study. *Eur J Orthod.* Aug 2005;27(4):355-362.
8. Ferrario VF, Sforza C, Serrao G, Ciusa V, Dellavia C. Growth and aging of facial soft tissues: A computerized three-dimensional mesh diagram analysis. *Clin Anat.* Sep 2003;16(5):420-433.
9. Sanders JE, Mitchell SM, Zachariah SG, Wu K. A digitizer with exceptional accuracy for use in prosthetics research: A technical note. *J Rehabil Res Dev.* 2003;40(2):191-196.
10. Bergmeir C, Seitel M, Frank C, De Simone R, Meinzer HP, Wolf I. Comparing calibration approaches for 3D ultrasound probes. *Int J Comput Assist Radiol Surg.* Mar 2009;4(2):203-213.
11. Benington PC, Gardener JE, Hunt NP. Masseter muscle volume measured using ultrasonography and its relationship with facial morphology. *Eur J Orthod.* Dec 1999;21(6):659-670.
12. Ezure T, Amano S. Influence of subcutaneous adipose tissue mass on dermal elasticity and sagging severity in lower cheek. *Skin Res Technol.* Aug 2010;16(3):332-338.
13. Sholts SB, Warmlander SK, Flores LM, Miller KW, Walker PL. Variation in the measurement of cranial volume and surface area using 3D laser scanning technology. *J Forensic Sci.* Jul 2010;55(4):871-876.
14. Kovacs L, Zimmermann A, Brockmann G, et al. Three-dimensional recording of the human face with a 3D laser scanner. *J Plast Reconstr Aesthet Surg.* 2006;59(11):1193-1202.

15. Edgar D, Day R, Briffa NK, Cole J, Wood F. Volume measurement using the Polhemus FastSCAN 3D laser scanning: a novel application for burns clinical research. *J Burn Care Res.* Nov-Dec 2008;29(6):994-1000.
16. Sforza C, Elamin F, Rosati R, Lucchini MA, De Menezes M, Ferrario VF. Morphometry of the ear in North Sudanese subjects with Down syndrome. A three-dimensional computerized assessment. *J Craniofac Surg.* 2010;in press.
17. See MS, Roberts C, Nduka C. Age- and gravity-related changes in facial morphology: 3-dimensional analysis of facial morphology in mother-daughter pairs. *J Oral Maxillofac Surg.* Jul 2008;66(7):1410-1416.
18. Weinberg SM, Naidoo S, Govier DP, Martin RA, Kane AA, Marazita ML. Anthropometric precision and accuracy of digital three-dimensional photogrammetry: comparing the Genex and 3dMD imaging systems with one another and with direct anthropometry. *J Craniofac Surg.* May 2006;17(3):477-483.
19. Wong JY, Oh AK, Ohta E, et al. Validity and reliability of craniofacial anthropometric measurement of 3D digital photogrammetric images. *Cleft Palate Craniofac J.* May 2008;45(3):232-239.
20. Dahlberg G. Statistical methods for medical and biological students. *New York: Interscience Publications.* 1940.
21. Vander Pluym J, Shan WW, Taher Z, et al. Use of magnetic resonance imaging to measure facial soft tissue depth. *Cleft Palate Craniofac J.* Jan 2007;44(1):52-57.
22. de Menezes M, Rosati R, Allievi C, Sforza C. A photographic system for the three-dimensional study of facial morphology. *Angle Orthod.* Nov 2009;79(6):1070-1077.
23. de Menezes M, Rosati R, Ferrario VF, Sforza C. Accuracy and reproducibility of a 3-dimensional stereophotogrammetric imaging system. *J Oral Maxillofac Surg.* Sep 2010;68(9):2129-2135.
24. Ferrario VF, Sforza C. Anatomy of emotion: a 3D study of facial mimicry. *Eur J Histochem.* 2007;51 Suppl 1:45-52.
25. Ferrario VF, Sforza C, Colombo A, Dellavia C, Dimaggio FR. Three-dimensional hard tissue palatal size and shape in human adolescents and adults. *Clin Orthod Res.* Aug 2001;4(3):141-147.
26. Ferrario VF, Sforza C, Poggio CE, Schmitz JH. Soft-tissue facial morphometry from 6 years to adulthood: a three-dimensional growth study using a new modeling. *Plast Reconstr Surg.* Mar 1999;103(3):768-778.
27. Rosati R, De Menezes M, Rossetti A, Sforza C, Ferrario VF. Digital dental cast placement in 3-dimensional, full-face reconstruction: a technical evaluation. *Am J Orthod Dentofacial Orthop.* Jul 2010;138(1):84-88.

28. Sforza C, Grandi G, De Menezes M, Tartaglia GM, Ferrario VF. Age- and sex-related changes in the normal human external nose. *Forensic Sci Int.* Aug 20 2010.
29. Sforza C, Peretta R, Grandi G, Ferronato G, Ferrario VF. Three-dimensional facial morphometry in skeletal Class III patients. A non-invasive study of soft-tissue changes before and after orthognathic surgery. *Br J Oral Maxillofac Surg.* Mar 2007;45(2):138-144.
30. Douglas TS. Image processing for craniofacial landmark identification and measurement: a review of photogrammetry and cephalometry. *Comput Med Imaging Graph.* Oct 2004;28(7):401-409.
31. Ghoddousi H, Edler R, Haers P, Wertheim D, Greenhill D. Comparison of three methods of facial measurement. *Int J Oral Maxillofac Surg.* Mar 2007;36(3):250-258.
32. Hammond P. The use of 3D face shape modelling in dysmorphology. *Arch Dis Child.* Dec 2007;92(12):1120-1126.
33. Sforza C, Dimaggio FR, Dellavia C, Grandi G, Ferrario VF. Two-dimensional vs three-dimensional assessment of soft tissue facial profile: a non invasive study in 6-year-old healthy children. *Minerva Stomatol.* May 2007;56(5):253-265.
34. Winder RJ, Darvann TA, McKnight W, Magee JD, Ramsay-Baggs P. Technical validation of the Di3D stereophotogrammetry surface imaging system. *Br J Oral Maxillofac Surg.* Jan 2008;46(1):33-37.
35. Bister D, Edler RJ, Tom BD, Prevost AT. Natural head posture--considerations of reproducibility. *Eur J Orthod.* Oct 2002;24(5):457-470.
36. Khambay B, Nairn N, Bell A, Miller J, Bowman A, Ayoub AF. Validation and reproducibility of a high-resolution three-dimensional facial imaging system. *Br J Oral Maxillofac Surg.* Jan 2008;46(1):27-32.
37. Majid Z CA, Ahmad A, Setan H,. Photogrammetry and 3D laser scanning as spatial data capture techniques for a national craniofacial database. *Photogramm Rec.* 2005;20:48-68.
38. Sawyer AR, See M, Nduka C. 3D stereophotogrammetry quantitative lip analysis. *Aesthetic Plast Surg.* Jul 2009;33(4):497-504.
39. Hajeer MY, Ayoub AF, Millett DT, Bock M, Siebert JP. Three-dimensional imaging in orthognathic surgery: the clinical application of a new method. *Int J Adult Orthodon Orthognath Surg.* 2002;17(4):318-330.
40. Ayoub A, Garrahy A, Hood C, et al. Validation of a vision-based, three-dimensional facial imaging system. *Cleft Palate Craniofac J.* Sep 2003;40(5):523-529.
41. Hammond P, Hutton TJ, Allanson JE, et al. 3D analysis of facial morphology. *Am J Med Genet A.* May 1 2004;126A(4):339-348.

42. Sforza C, Dellavia C, Goffredi M, Ferrario VF. Soft tissue facial angles in individuals with ectodermal dysplasia: A three-dimensional noninvasive study. *Cleft Palate Craniofac J.* May 2006;43(3):339-349.
43. Toma AM, Zhurov A, Playle R, Ong E, Richmond S. Reproducibility of facial soft tissue landmarks on 3D laser-scanned facial images. *Orthod Craniofac Res.* Feb 2009;12(1):33-42.
44. Maal TJ, Plooij JM, Rangel FA, Mollemans W, Schutyser FA, Berge SJ. The accuracy of matching three-dimensional photographs with skin surfaces derived from cone-beam computed tomography. *Int J Oral Maxillofac Surg.* Jul 2008;37(7):641-646.
45. Ozsoy U, Demirel BM, Yildirim FB, Tosun O, Sarikcioglu L. Method selection in craniofacial measurements: advantages and disadvantages of 3D digitization method. *J Craniomaxillofac Surg.* Jul 2009;37(5):285-290.
46. Plooij JM, Swennen GR, Rangel FA, et al. Evaluation of reproducibility and reliability of 3D soft tissue analysis using 3D stereophotogrammetry. *Int J Oral Maxillofac Surg.* Mar 2009;38(3):267-273.
47. Sforza C, Grandi G, Binelli M, Tommasi DG, Rosati R, Ferrario VF. Age- and sex-related changes in the normal human ear. *Forensic Sci Int.* May 30 2009;187(1-3):110 e111-117.
48. Toma AM, Zhurov A, Playle R, Richmond S. A three-dimensional look for facial differences between males and females in a British-Caucasian sample aged 151/2 years old. *Orthod Craniofac Res.* Aug 2008;11(3):180-185.
49. Rangel FA, Maal TJ, Berge SJ, et al. Integration of digital dental casts in 3-dimensional facial photographs. *Am J Orthod Dentofacial Orthop.* Dec 2008;134(6):820-826.
50. Aldridge K, Boyadjiev SA, Capone GT, DeLeon VB, Richtsmeier JT. Precision and error of three-dimensional phenotypic measures acquired from 3dMD photogrammetric images. *Am J Med Genet A.* Oct 15 2005;138A(3):247-253.
51. Krimmel M, Kluba S, Bacher M, Dietz K, Reinert S. Digital surface photogrammetry for anthropometric analysis of the cleft infant face. *Cleft Palate Craniofac J.* May 2006;43(3):350-355.
52. Sforza C, Peretta R, Grandi G, Ferronato G, Ferrario VF. Soft tissue facial planes and masticatory muscle function in skeletal Class III patients before and after orthognathic surgery treatment. *J Oral Maxillofac Surg.* Apr 2008;66(4):691-698.
53. Kau CH, Richmond S, Incrapera A, English J, Xia JJ. Three-dimensional surface acquisition systems for the study of facial morphology and their application to maxillofacial surgery. *Int J Med Robot.* Jun 2007;3(2):97-110.
54. Celik E, Polat-Ozsoy O, Toygar Memikoglu TU. Comparison of cephalometric measurements with digital versus conventional cephalometric analysis. *Eur J Orthod.* Jun 2009;31(3):241-246.

55. Moro A, Correra P, Boniello R, Gasparini G, Pelo S. Three-dimensional analysis in facial asymmetry: comparison with model analysis and conventional two-dimensional analysis. *J Craniofac Surg.* Mar 2009;20(2):417-422.
56. Calzolari E, Pierini A, Astolfi G, Bianchi F, Neville AJ, Rivieri F. Associated anomalies in multi-malformed infants with cleft lip and palate: An epidemiologic study of nearly 6 million births in 23 EUROCAT registries. *Am J Med Genet A.* Mar 15 2007;143(6):528-537.
57. Oberoi S, Chigurupati R, Vargervik K. Morphologic and management characteristics of individuals with unilateral cleft lip and palate who required maxillary advancement. *Cleft Palate Craniofac J.* Jan 2008;45(1):42-49.
58. Ferrario VF, Sforza C, Schmitz JH, Colombo A. Quantitative description of the morphology of the human palate by a mathematical equation. *Cleft Palate Craniofac J.* Sep 1998;35(5):396-401.
59. Restrepo CC, Sforza C, Colombo A, Pelaez-Vargas A, Ferrario VF. Palate morphology of bruxist children with mixed dentition. A pilot study. *J Oral Rehabil.* May 2008;35(5):353-360.
60. Baek SH, Son WS. Difference in alveolar molding effect and growth in the cleft segments: 3-dimensional analysis of unilateral cleft lip and palate patients. *Oral Surg Oral Med Oral Pathol Oral Radiol Endod.* Aug 2006;102(2):160-168.
61. Boldt F, Weinzierl C, Hertrich K, Hirschfelder U. Comparison of the spatial landmark scatter of various 3D digitalization methods. *J Orofac Orthop.* May 2009;70(3):247-263.
62. Braumann B, Keilig L, Bourauel C, Niederhagen B, Jager A. 3-dimensional analysis of cleft palate casts. *Ann Anat.* Jan 1999;181(1):95-98.
63. Littlefield TR, Cherney JC, Luisi JN, Beals SP, Kelly KM, Pomatto JK. Comparison of plaster casting with three-dimensional cranial imaging. *Cleft Palate Craniofac J.* Mar 2005;42(2):157-164.
64. He X, Shi B, Jiang S, Li S, Zheng Q, Yan W. 110 infants with unrepaired unilateral cleft lip: An anthropometric analysis of the lip and nasal deformities. *Int J Oral Maxillofac Surg.* Sep 2010;39(9):847-852.
65. Kecik D, Enacar A. Effects of nasoalveolar molding therapy on nasal and alveolar morphology in unilateral cleft lip and palate. *J Craniofac Surg.* Nov 2009;20(6):2075-2080.
66. Oosterkamp BC, van der Meer WJ, Rutenfrans M, Dijkstra PU. Reliability of linear measurements on a virtual bilateral cleft lip and palate model. *Cleft Palate Craniofac J.* Sep 2006;43(5):519-523.
67. Bilwatsch S, Kramer M, Haeusler G, et al. Nasolabial symmetry following Tennison-Randall lip repair: a three-dimensional approach in 10-year-old patients with unilateral clefts of lip, alveolus and palate. *J Craniomaxillofac Surg.* Jul 2006;34(5):253-262.

68. Chen PK, Por YC, Liou E, Chang FC. Maxillary Distraction Osteogenesis in the Adolescent Cleft Patient. 3-Dimensional Computed Tomography Analysis of Linear and Volumetric Changes over 5 Years. *Cleft Palate Craniofac J.* Jun 10 2010.
69. Naidu D, Scott J, Ong D, Ho CT. Validity, reliability and reproducibility of three methods used to measure tooth widths for bolton analyses. *Aust Orthod J.* Nov 2009;25(2):97-103.
70. Suzuki A, Takenoshita Y, Honda Y, Matsuura C. Dentocraniofacial morphology in parents of children with cleft lip and/or palate. *Cleft Palate Craniofac J.* Mar 1999;36(2):131-138.
71. Nagy K, Mommaerts MY. Analysis of the cleft-lip nose in submental-vertical view, Part I--reliability of a new measurement instrument. *J Craniomaxillofac Surg.* Sep-Oct 2007;35(6-7):265-277.
72. De Menezes M, Sforza C. Three-dimensional face morphometry. *Dental Press J. Orthod.* 2010;15(1):13-15.

8. WEBOGRAPHY

I. http://ucsdultrasound.com/yahoo_site_admin/assets/images/ultrasound_transducers.24673744_large.jpg (October, 2010)

II. http://www.polhemus.com/?page=Scanning_Fastscan (October, 2010)

III. http://cadcamdentale.com/scanner_dentale.html (October, 2010)

9. FIGURES

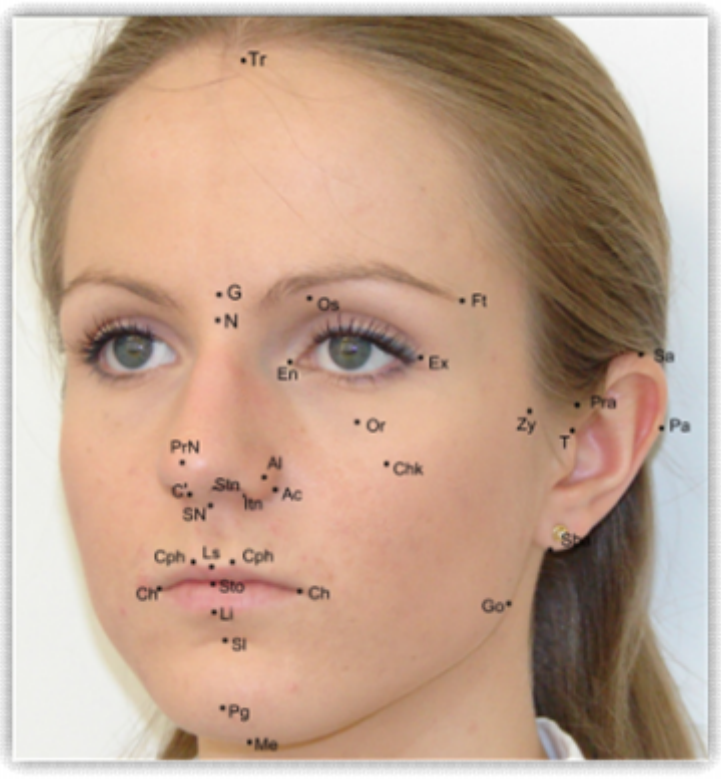

Figure 1 – Soft tissue facial landmarks digitized on all subjects[22]

Figure 2 – Electromechanical digitizer

Figure 3 – Electromagnetic digitizer

Figure 4 – Ultrasound Probes [I]

Figure 5 (a^{II},b^{III}) – Laser scanner

Figure 6 –3D reproduction - facial surface rendering

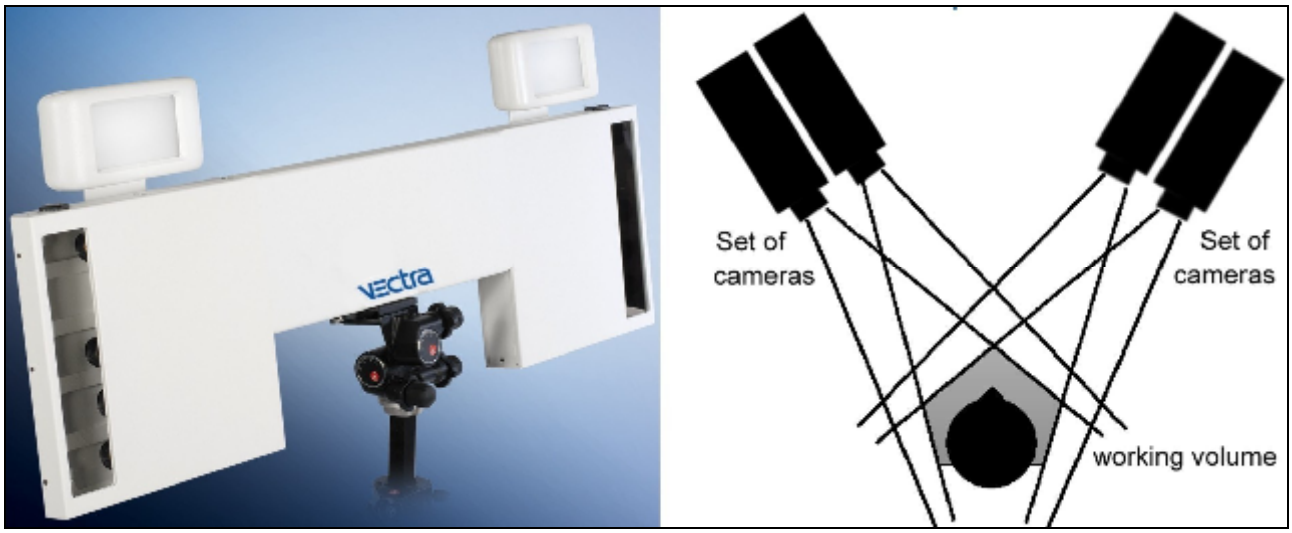

Figure 7 – Stereophotogrammetric system - Vectra 3D [72]

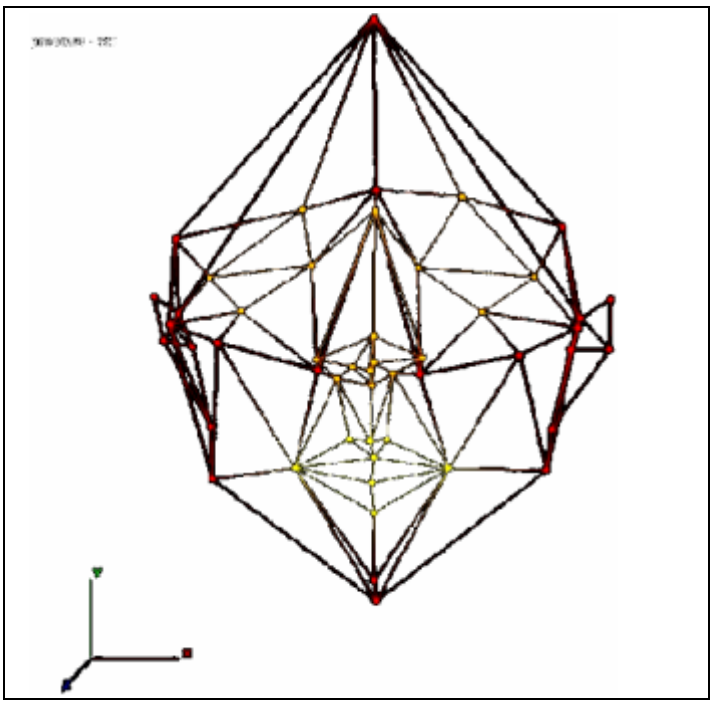

Figure 8 - Facial geometric model obtained with 50 landmarks digitized using the electromagnetic digitizer (Polhemus)[22]

Figure 9 – Example of photograph taken at different angles.[22]

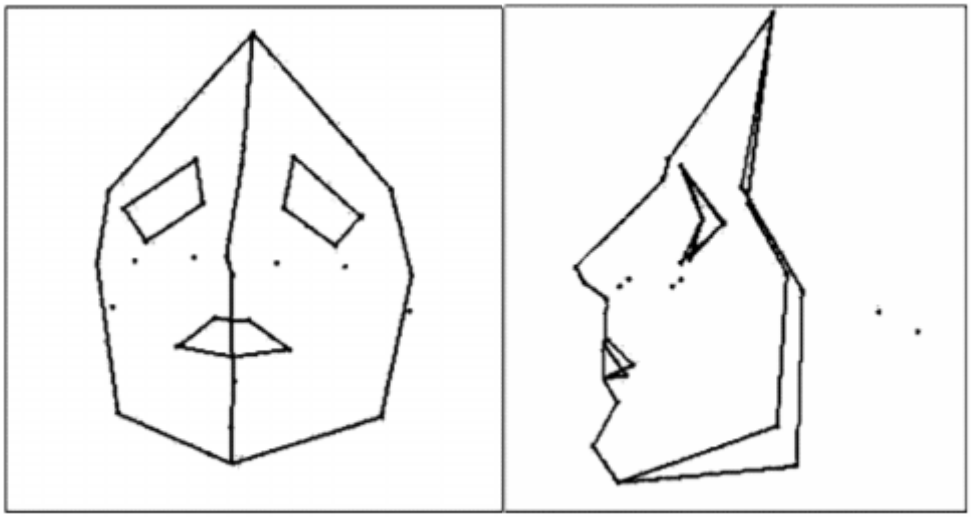

Figure 10 – Facial geometric model obtained with 36 landmarks digitized using the Photomodeler software[22]

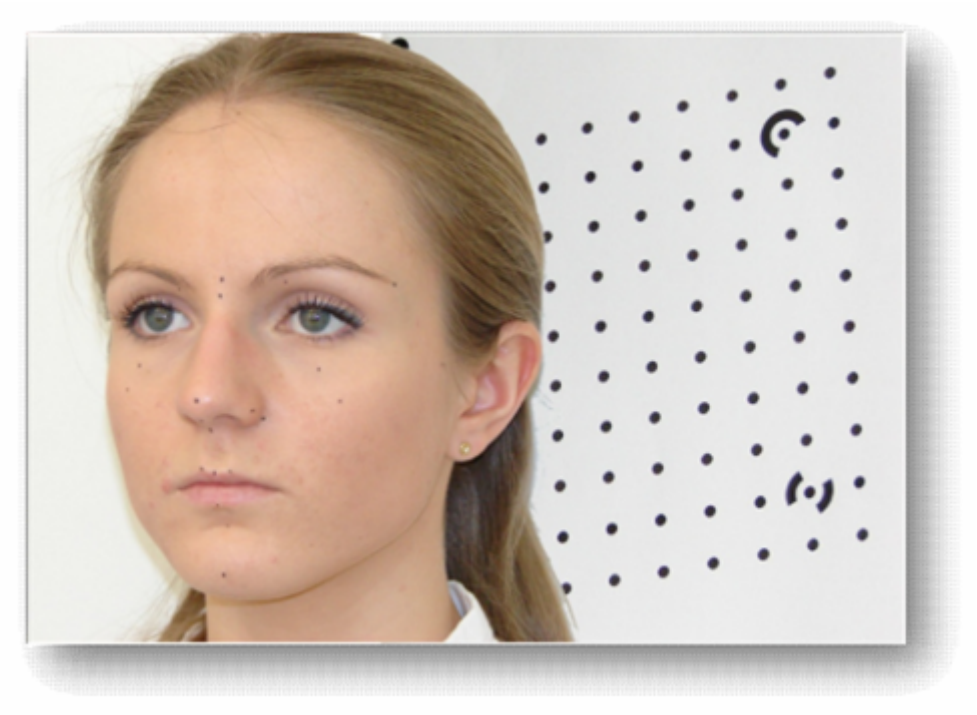

Figure 11– Photomodeler guide paper [22]

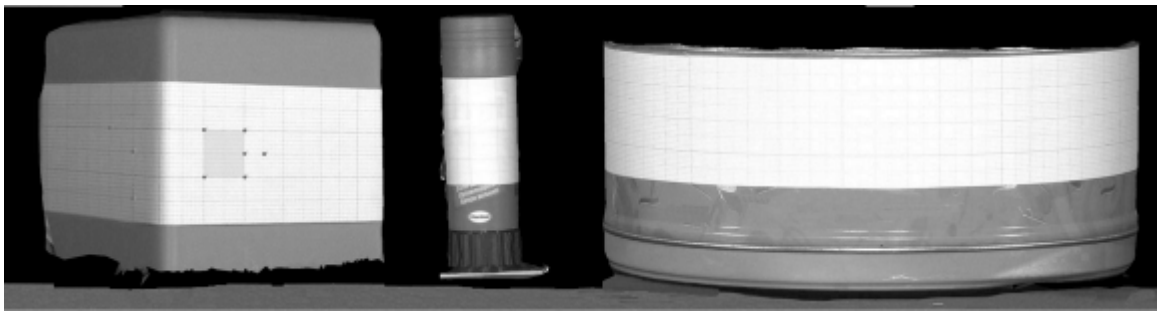

Figure 12 – Standard objects with the measuring grid

Figure 13 – Two sets of 3D facial reconstructions made by stereophtogrammetry: open lips (with cheek retractors) and closed lips

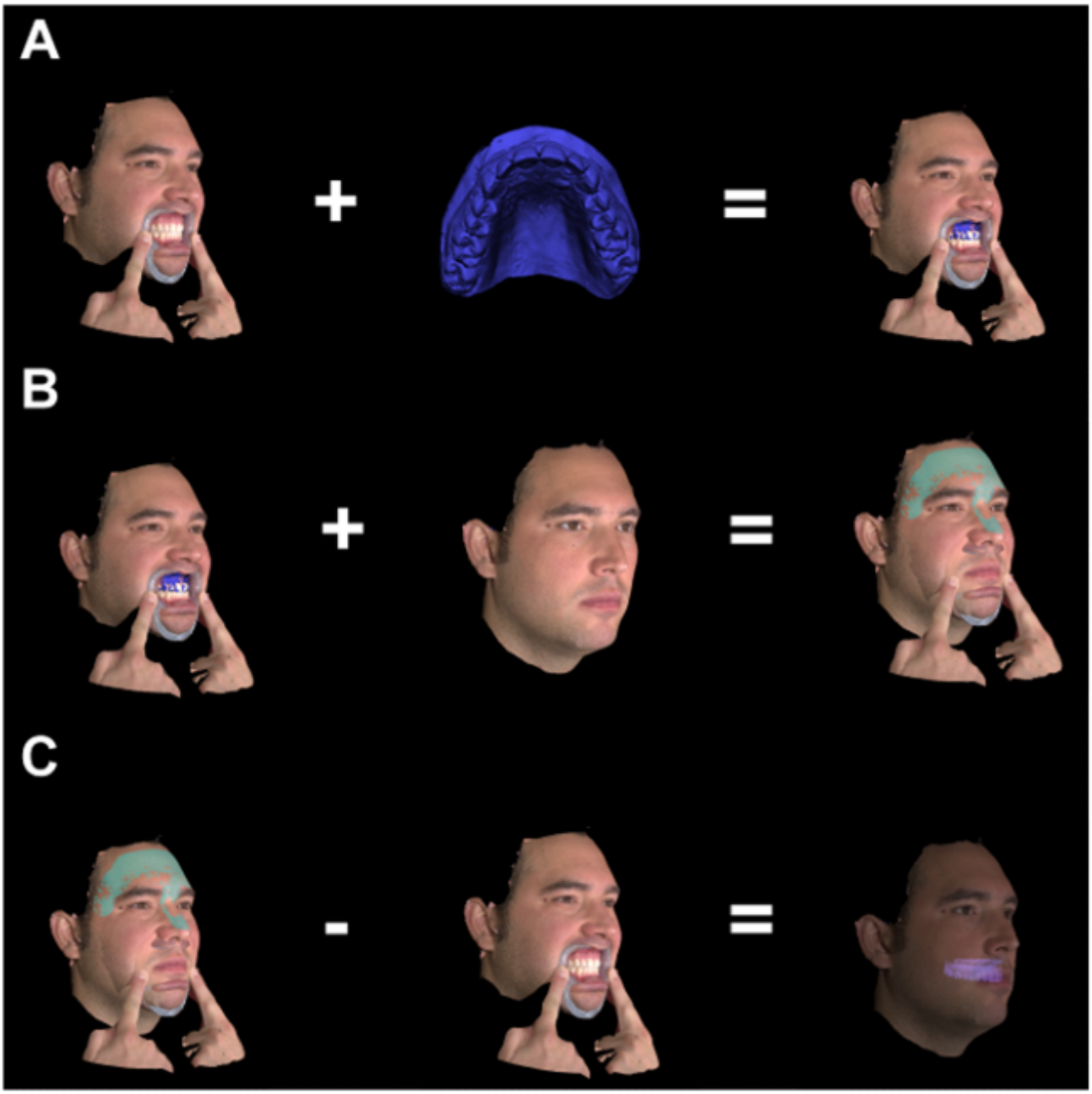

Figure 14 - Facial and dental file matching steps[27]

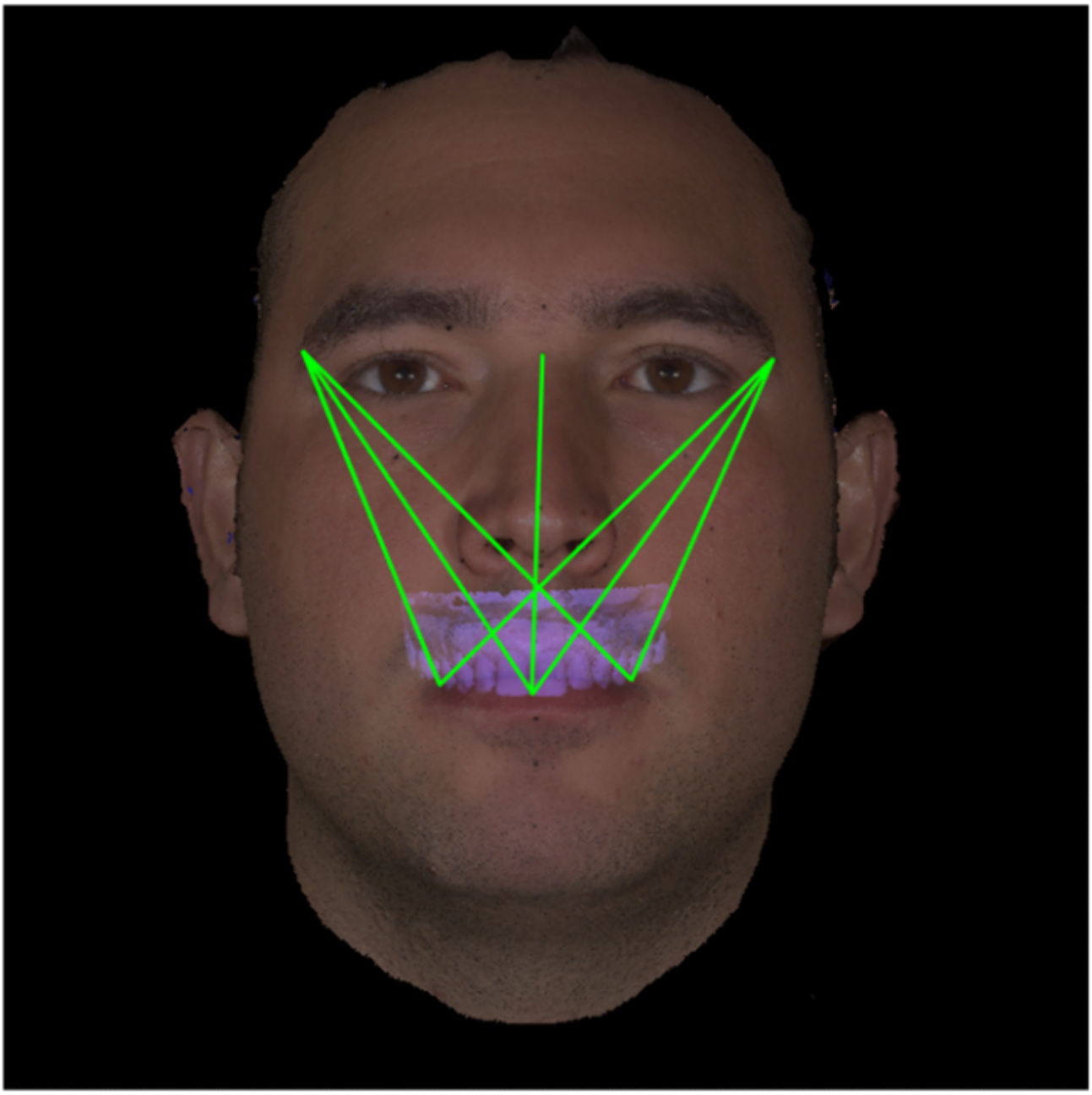

Figure 15. Linear distances from cutaneous and dental landmarks performed on the virtual reproduction[27]

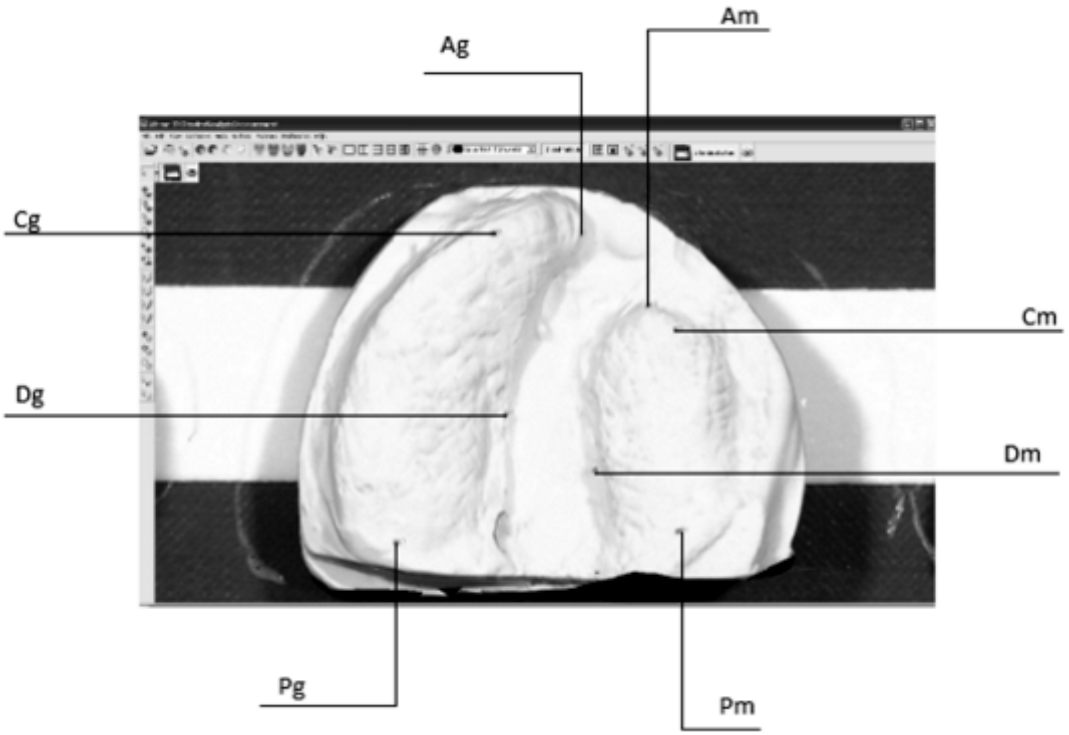

Figure 16 –Landmark position on the UCLP casts

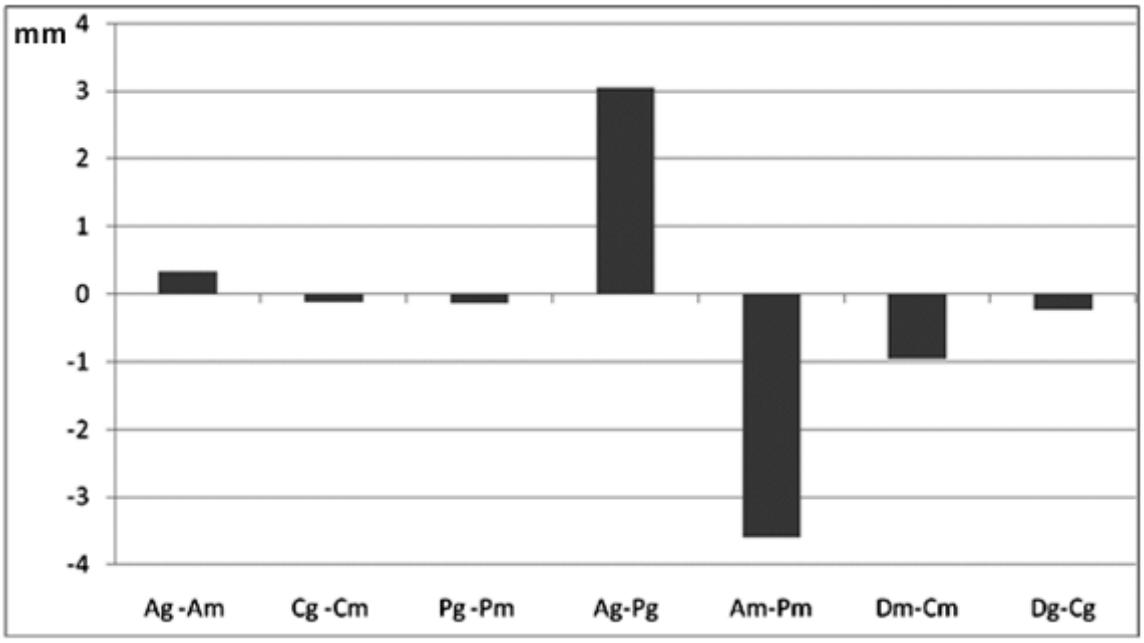

Figure 17 – Difference between 3D stereophotogrammetry and caliper measurements;
Positive values mean 3D stereophotogrammetry overestimation; Negative values mean caliper overestimation.

10. TABLES

Table 1 - Analyzed distances and angles

Distance	Angle
Ex*r* – Ex*l* *	N-Sn-Pg
T *r* – T *l* *	Sl-N-Sn
Go*r* - Go*l**	T*r*-N-T *l* *
Ch *r* – Ch *l**	T*r*-Pn-T *l**
Tr – N	T *r*-Pg-T *l**
N – Sn	Ex *r*-N-Ex *l* *
Sn – Pg	Go *r*- Pg-Go *l**
N - Pg	T *r*-Go *r*-Pg *
N - (T *r*—T *l*) *	T *l* –Go *l*-Pg*
Sn - (T *r*—T *l)* *	N-Prn-Pg
Pg – (T *r*—T *l*) *	Sn -N-Prn
Pg - (Go*r* - Go*l*) *	(T *r* - Al *r*) - (Go *r* - Pg) *
Tr-Go	(T *l* –Al *l*) - (Go *l* - Pg) *
Ls - (Prn-Pg):	(T-N) - (Go-Pg)
Li - (Prn-Pg):	Prn- Sn –Ls
	Li-Sl-Pg
	(Sn -Ls)-(Li-Pg)
	(Sn -Ls)-Li-Sl)

** l – Left r – Right*

Table 2 – Means and Standard Deviations (SD) across linear distances (mm), mean absolute differences (MAD) and *p* value

Distances	E. digitizer		Photo			
	Mean	SD	Mean	SD	MAD	*p* value **
Ex*r*-Ex*l*∞	90.5	5.23	91.12	5.69	0.62	0.07 (ns)
T*r*-T*l*∞	141.85	7.92	144.52	7.54	2.67	0.01*
Go*r*-Go*l*∞	116.16	9.23	117.78	7.91	1.62	0.07 (ns)
Ch*r*-Ch*l*∞	47.13	5.1	47.81	5.97	0.68	0.32 (ns)
Tr-N	67.44	7.99	67.03	8.52	0.41	0.31 (ns)
N-Sn	53.23	3.71	52.95	3.7	0.28	0.27 (ns)
Sn-Pg	57.13	3.75	56.75	4.05	0.38	0.27 (ns)
N-Pg	108.43	5.87	108.35	6.12	0.08	0.83 (ns)
N-T	98.59	4.59	97.9	4.55	0.69	0.10 (ns)
Sn-T	107.84	5.82	106.83	6.22	1.01	0.16 (ns)
Pg-T	125.48	8.84	122.96	9.08	2.52	0.02*
Pg-Go	78.16	5.25	78.21	5.86	0.05	0.95 (ns)
T-Go	64.98	7.58	63.41	7.65	1.57	0.11 (ns)
Ls - (Prn-Pg)	5.62	1.55	5.64	1.47	0.02	0.93 (ns)
Li - (Prn-Pg)	3.96	1.97	3.99	1.91	0.03	0.91 (ns)

∞ *r: right - l left* (ns)- not significant difference, p > 0.05

*Statistically significant *p* values ** Paired *t*-test *p* values comparing electromagnetic digitizer and PhotoModeler

Table 3 – Means and Standard Deviations (SD) across angles (º), mean absolute differences (MAD) and *p* value

Angles	E. digitizer		Photo			
	Mean	SD	Mean	SD	MAD	*p* v*alue* **
N-sn-Pg	159.07	3.71	159.45	3.86	0.38	0.08 (ns)
Sl-N-Sn	12.05	1.76	11.87	2.03	0.18	0.49 (ns)
T*r*-N-T*l*∞	71.04	2.96	72.56	2.95	1.52	0.03*
T*r*-Prn-T*l*∞	60.23	2.14	62.04	2.69	1.81	0.01*
T*r*-Pg-T*l*∞	58.92	2.36	60.43	3.02	1.51	0.04*
Ex*r*-N-Ex*l*∞	116.20	5.37	118.71	6.43	2.51	0.052(ns)
Go*r*-Pg-Go*l*∞	73.66	3.24	74.19	3.05	0.53	0.65(ns)
T*r*-Go*r*-Pg∞	125.63	5.61	125.92	6.26	0.29	0.67(ns)
T*l*-Go*l*-Pg∞	124.74	4.97	124.67	5.67	0.07	0.87(ns)
N-Prn-Pg	126.59	3.11	127.17	3.53	0.58	0.07(ns)
Sn-N-Prn	21.70	1.59	21.35	1.65	0.35	0.08(ns)
(T*r*-Alar)-(Go*r*-Pg) ∞	11.52	1.87	11.79	2.58	0.27	0.56(ns)
(T*l*-Alal)-(Go*l*-Pg) ∞	9.98	2.91	9.69	2.5	0.29	0.62(ns)
(T-N)-(Go-Pg)	32.24	5.56	33.07	5.43	0.83	0.11(ns)
Prn-SN-Ls	125.55	8.79	125.46	7.52	0.09	0.95(ns)
Li-Sl-Pg	132.74	11.93	133.56	11.43	0.82	0.76(ns)
(Sn-Ls)-(Li-Pg)	165.14	9.14	164.96	8.52	0.18	0.92(ns)
(Sn-Ls)-(Li-Sl)	140.54	15.95	140.55	12.21	0.01	1.00(ns)

∞ *r: right - l left* (ns)- not significant difference, p > 0.05

*Statistically significant *p* values ** Paired *t*-test *p* values comparing electromagnetic digitizer and PhotoModeler

Table 4 – Error analysis: reproducibility of the tracings, re-performed at 1 month interval

Distances (mm)	Error n = 3	*p* Value	Angles (º)	Error n = 3	*p* Value
Exr-Exl	1.57	0.07	N-Sn-Pg	0.25	0.17
Tr-Tl	0.97	0.51	B-N-Sn	0.10	0.17
Gor-Gol	0.23	0.85	Tr-N-Tl	1.12	0.62
Chr-Chl	0.74	0.38	Tr-Prn-Tl	1.16	0.48
Tr-N	0.25	0.79	Tr-Pg-Tl	1.03	0.35
N-Sn	0.55	0.32	Exr-N-Exl	2.84	0.16
Sn-Pg	0.29	0.64	Gor-Pg-Gol	2.61	0.24
N-Pg	0.13	0.83	Tr-Gor-Pg	1.05	0.74
N-T	0.42	0.64	Tl-Gol-Pg	0.54	0.97
Sn-T	0.23	0.78	N-Prn-Pg	0.20	0.37
Pg-T	0.28	0.78	Sn-N-Prn	0.11	0.18
Pg-Go	0.90	0.68	(Trr-Alar)-(Gor-Pg)	1.45	0.55
T-Go	0.19	0.89	(Trl-Alal)-(Gol-Pg)	1.14	0.38
Ls - (Prn-Pg)	0.50	0.51	(Tr-N)-(Go-Pg)	0.59	0.15
Li - (Prn-Pg):	0.21	0.28	Prn-Sn-Ls	0.72	0.18
			Li-Sl-Pg	2.02	0.72
			(Sn-Ls)-(Li-Pg)	2.10	0.66
			(Sn-Ls)-(Li-Sl)	1.92	0.34

(mm) – millimeter (º) –degree Technical error of measurement (TEM) and systematic error (*p* value)
All p values are not significant, p > 0.05.

Table 5 – Error analysis: reproducibility during subject rearrangement

Distances (mm)	Error n = 3	*p* value	Angles (º)	Error n = 3	*p* value
Exr-Exl	3.91	0.13	N-Sn-Pg	1.52	0.53
Tr-Tl	5.26	0.20	B-N-Sn	0.82	0.49
Gor-Gol	3.24	0.19	Tr-N-Tl	4.02	0.95
Chr-Chl	2.39	0.26	Tr-Prn-Tl	3.76	0.87
Tr-N	1.11	0.64	Tr-Pg-Tl	3.03	0.84
N-Sn	1.09	0.43	Exr-N-Exl	5.14	0.46
Sn-Pg	2.70	0.07	Gor-Pg-Gol	4.41	0.73
N-Pg	3.86	0.15	Tr-Gor-Pg	3.63	0.31
N-T	3.65	0.46	Tl-Gol-Pg	4.26	0.34
Sn-T	2.02	0.75	N-Prn-Pg	3.08	0.73
Pg-T	2.58	0.65	Sn-N-Prn	0.71	0.44
Pg-Go	3.53	0.42	(Trr-Alar)-(Gor-Pg)	1.77	0.18
T-Go	0.48	0.78	(Trl-Alal)-(Gol-Pg)	1.67	0.86
Ls - (Prn-Pg)	0.31	0.61	(Tr-N)-(Go-Pg)	2.27	0.57
Li - (Prn-Pg):	0.99	0.21	Prn-Sn-Ls	4.22	0.34
			Li-Sl-Pg	5.58	0.16
			(Sn-Ls)-(Li-Pg)	0.67	0.38
			(Sn-Ls)-(Li-Sl)	5.61	0.12

(mm) – millimeter (º) –degree Technical error of measurement (TEM) and *systematic error (p* value)
All p values are not significant, p > 0.05.

Table 6 - Analyzed soft tissue facial distances.

Distances	
Ex*r*-Ex*l*/*	upper facial width
T*r*-T*l*/*	middle facial width
Zy*r*- Zy*l*/*	interzygion distance
Go*r*-Go*l*/*	lower facial width
Ch*r*-Ch*l*/*	mouth width
Tr-N	forehead height
N-Sn	anterior upper facial height
Sn-Pg	anterior lower facial height
N-Pg	anterior facial height
T-Go	posterior facial height
N-T	upper facial depth
Sn-T	middle facial depth
Pg-T	lower facial depth
Pg-Go	mandibular corpus length
Ls - (Prn-Pg)	upper lip to E-line distance
Li - (Prn-Pg)	lower lip to E-line distance

* right and left side noted as “r” and “l” respectively

Table 7.- Accuracy of the stereophotogrammetric system.

		Real values	**Measured values**	**Accuracy error (%)**
Cubic box	Distances (mm)	10	10.02	0.20
	Angles (deg)	90	89.96	0.04
	Area (cm^2)	1	1.01	0.10
Small cylindrical object	Distances (mm)	3	3.02	1.21
	Angles (deg)	90	88.95	1.17
	Area (cm^2)	3	2.99	0.28
Big cylindrical object	Distances (mm)	34	34.02	0.05
	Angles (deg)	90	89.23	0.86
	Area (cm^2)	68	67.59	0.60

Table 8 - Differences between separate calibrations of the stereophotogrammetric analyzer.

	1st calibration		2nd calibration		Mean			
Distances	Mean	SD	Mean	SD	difference	p value	MAD	TEM
Ex*r*-Ex*l*	90.26	3.92	91.21	3.40	-0.05	0.84	0.61	0.52
T*r*-T*l*	142.37	8.23	142.29	8.14	-0.08	0.42	0.26	0.21
Go*r*-Go*l*	114.84	8.03	114.91	7.39	0.07	0.85	0.85	0.79
Zy *r*- Zy *l*	138.92	7.97	138.89	7.98	-0.03	0.42	0.08	0.08
Ch*r*-Ch*l*	47.77	3.88	47.47	4.66	-0.30	0.56	1.19	1.08
Tr-N	67.33	9.40	67.40	9.08	0.07	0.71	0.37	0.42
N-Sn	57.78	3.15	57.85	3.15	0.07	0.19	0.13	0.12
Sn-Pg	56.02	3.11	56.15	3.19	0.13	0.63	0.67	0.58
N-Pg	112.11	3.87	112.32	3.76	0.21	0.39	0.65	0.52
T-Go	65.19	6.73	65.13	6.58	-0.06	0.76	0.39	0.40
N-T	100.13	5.63	100.26	5.52	0.13	0.44	0.29	0.35
Sn-T	107.79	5.89	107.72	5.60	-0.07	0.63	0.30	0.31
Pg-T	125.10	7.74	124.99	7.18	-0.11	0.64	0.56	0.46
Pg-Go	77.11	6.84	76.87	6.97	-0.23	0.54	0.87	0.81
Ls - (Prn-Pg)	6.12	2.07	6.00	2.07	-0.05	0.63	0.20	0.19
Li - (Prn-Pg)	3.94	2.57	3.89	2.52	-0.05	0.62	0.24	0.21

All values are mm
MAD: mean absolute difference
TEM: Technical error of measurement
p values from paired Student's t tests. All p values are not significant, $p > 0.05$.

Table 9 - Differences between operators.

	1st operator		2nd operator		Mean			
Distances	Mean	SD	Mean	SD	difference	p value	MAD	TEM
Ex*r*-Ex*l*	91.26	3.92	91.26	3.60	0.00	0.99	0.74	0.63
T*r*-T*l*	142.37	8.23	142.38	8.24	-0.01	0.89	0.14	0.15
Go*r*-Go*l*	114.83	8.07	114.98	8.00	-0.16	0.10	0.22	0.21
Zy *r*- Zy *l*	138.92	7.97	138.89	7.94	0.03	0.22	0.05	0.05
Ch*r*-Ch*l*	47.77	3.88	47.84	3.51	-0.07	0.86	0.90	0.81
Tr-N	67.33	9.40	67.29	9.52	0.04	0.82	0.31	0.31
N-Sn	57.84	3.11	57.96	3.20	-0.12	0.16	0.21	0.19
Sn-Pg	56.02	3.11	55.88	3.24	0.14	0.13	0.23	0.20
N-Pg	112.11	3.87	112.20	3.84	-0.09	0.41	0.20	0.24
T-Go	65.19	6.73	65.03	6.50	0.16	0.29	0.35	0.32
N-T	100.13	5.63	100.18	5.66	-0.05	0.73	0.31	0.30
Sn-T	107.79	5.89	107.83	5.69	-0.04	0.83	0.40	0.39
Pg-T	125.10	7.74	125.09	7.51	0.00	0.98	0.37	0.36
Pg-Go	77.11	6.84	77.08	6.83	0.03	0.60	0.11	0.10
Ls - (Prn-Pg)	6.12	2.07	6.11	2.00	0.01	0.75	0.07	0.07
Li - (Prn-Pg)	3.94	2.57	3.92	2.52	0.03	0.52	0.10	0.08

All values are mm
MAD: mean absolute difference
TEM: Technical error of measurement
p values from paired Student's t tests ($p > 0.05$). All p values are not significant, $p > 0.05$.

Table 10. Differences between repeated acquisitions.

	1st acquisition		2nd acquisition		Mean			
Distances	Mean	SD	Mean	SD	difference	p value	MAD	TEM
Ex*r*-Ex*l*	91.49	4.12	91.13	3.94	0.36	0.06	0.52	0.43
T*r*-T*l*	142.43	8.32	142.31	8.14	0.12	0.27	0.28	0.23
Zy *r*- Zy *l*	138.95	7.98	138.89	7.97	0.06	0.17	0.10	0.09
Go*r*-Go*l*	114.63	8.16	115.09	8.20	-0.46	0.10	0.64	0.63
Ch*r*-Ch*l*	47.79	3.47	47.75	4.35	0.04	0.93	1.18	0.91
Tr-N	67.31	9.09	67.34	9.71	-0.03	0.91	0.49	0.52
N-Sn	57.76	3.08	57.83	3.20	-0.07	0.50	0.25	0.22
Sn-Pg	56.12	3.33	55.91	3.03	0.21	0.63	0.91	0.91
N-Pg	112.18	3.85	112.03	3.99	0.15	0.72	0.89	0.86
T-Go	65.31	6.55	65.07	6.93	0.24	0.32	0.48	0.51
N-T	100.10	5.55	100.16	5.71	-0.06	0.63	0.28	0.26
Sn-T	107.88	5.81	107.70	5.99	0.18	0.38	0.42	0.43
Pg-T	125.36	7.65	124.83	7.86	0.53	0.07	0.63	0.67
Pg-Go	77.20	6.82	76.91	6.87	0.29	0.39	0.81	0.71
Ls - (Prn-Pg)	6.14	2.04	6.09	2.11	0.05	0.63	0.25	0.22
Li - (Prn-Pg)	3.97	2.59	3.91	2.57	0.06	0.66	0.32	0.28

All values are mm
MAD: mean absolute difference
TEM: Technical error of measurement
p values from paired Student's t tests ($p > 0.05$). All p values are not significant, $p > 0.05$.

Table 11 - Analyzed distances.

Distances
Ft*r* - P*r*
Ft*r* - P*l*
N- I
Ft*l* - P*l*
Ft*l* - P*r*
Ft*r* - I
Ft*l* - I

In subscripts: l, left side; r, right side.

Table 12 - Differences between distance assessments.

Distances	In vivo (mm)		Virtual (mm)		MAD	TEM	REM	T-Test
	Mean	SD	Mean	SD	(mm)	(mm)	(%)	
Ft*r*-P*r*	86.9	6.5	87.0	6.1	0.8	0.7	0.9	0.71
Ft*r*-P*l*	106.7	4.1	106.9	3.4	1.1	1.0	1.0	0.65
N-I	85.8	19.9	86.3	20.1	0.7	0.6	0.9	0.04*
Ft*l*- P*l*	87.4	5.4	87.8	5.5	0.9	0.7	1.1	0.27
Ft*l*-P*r*	106.0	3.6	107.0	3.7	1.2	1.0	1.1	0.01*
Ft*r*-I	101.9	5.8	102.1	5.1	0.9	0.8	0.9	0.50
Ft*l*-I	100.8	5.9	101.8	5.9	1.2	1.0	1.2	0.02*

SD: standard deviation
MAD: mean absolute difference
TEM: technical error of measurement
REM: relative error magnitude
p values from paired Student's t tests; * denotes a significant value ($p < 0.05$).

Table 13 - Reproducibility of matching

	1st Match		2nd Match				
Distance (mm)	Media	SD	Media	SD	p value	MAD	TEM
Ft*r*-P*r*	88.26	5.32	88.27	5.31	0.92	0.26	0.21
Ft*r*-P*l*	106.83	4.49	106.89	4.64	0.79	0.53	0.46
N-I	98.05	25.01	97.92	24.89	0.30	0.31	0.25
Ft*l*- P*l*	88.24	5.04	88.33	5.35	0.72	0.58	0.52
Ft*l*-P*r*	106.67	3.98	106.74	4.21	0.63	0.33	0.27
Ft*r*-I	102.43	5.37	102.42	5.16	0.89	0.19	0.18
Ft*l*-I	102.11	6.41	101.99	6.35	0.30	0.28	0.24

MAD: mean absolute difference
TEM: Technical error of measurement
p values from paired Student's t tests ($p > 0.05$). All p values are not significant, $p > 0.05$.

Table 14 - Average distance of the 2 matched surfaces

Subjects	Average Distance (mm)	SD
1	0.35	0.14
2	0.04	0.16
3	0.46	0.22
4	0.1	0.07
5	0.19	0.16
6	1.1	0.2
7	0.16	0.17
8	0.6	0.15
9	0.42	0.32
10	0.36	0.09
11	0.58	0.2
Mean	0.40	0.17

Table 15. Reference points.

Segment	Landmarks	Abbreviation	Description
Greater	Postgingivale	Pg	Posterior end point of the alveolar crest
Greater	Anterior Alveolar	Ag	Anterior end point of the alveolar crest
Greater	Canine	Cg	The most prominent point of the canine area
Greater	Deep cleft	Dg	Deepest point of the clef
Minor	Postgingivale	Pm	Posterior end point of the alveolar crest
Minor	Anterior Alveolar	Am	Anterior end point of the alveolar crest
Minor	Canine	Cm	The most prominent point of the canine area
Minor	Deep cleft	Dm	Deepest point of the clef

Table 16. Measurement obtained in all casts.

Distances (mm)	Definition
Ag-Am	Anterior transverse cleft gap between the greater and the minor segments
Cg- Cm	Intercanine width between the greater and the minor cleft segments
Pg-Pm	Posterior transverse distance between the greater and the minor cleft segments
Ag-Pg	Length of the greater cleft segment
Am-Pm	Length of the minor cleft segment
Dm – Cm	Height of the greater cleft segment
Dg – Cg	Height of the minor cleft segment

Table 17. Differences between repeated acquisitions.

	A1		A2		Comparison			
Distances	Mean	SD	Mean	SD	p value	MAD	TEM	REM (%)
Ag -Am	7.44	3.85	7.37	3.89	0.11	0.09	0.27	1.18
Cg -Cm	21.73	4.76	21.65	4.89	0.45	0.32	0.67	1.49
Pg -Pm	31.62	3.10	31.67	3.05	0.35	0.27	0.35	0.86
Ag-Pg	30.19	3.18	30.15	3.13	0.10	0.15	0.19	0.62
Am-Pm	22.00	2.63	22.04	2.64	0.13	0.07	0.19	0.33
Dm-Cm	13.84	2.25	13.74	2.22	0.07	0.19	0.38	1.40
Dg-Cg	15.10	2.34	15.13	2.33	0.21	0.05	0.19	0.32

All values are mm MAD: mean absolute difference
TEM: Technical error of measurement
REM: relative error magnitude
p values from paired Student's t tests. All p values are not significant, $p > 0.05$.

Table 18. Comparison between linear distances obtained by stereophotogrammetry (Vectra system) and by caliper.

	Vectra		Caliper		Comparison			
Distances	Mean	SD	Mean	SD	p value	MAD	TEM	REM (%)
Ag -Am	7.44	3.85	7.10	3.76	0.00	0.56	0.49	7.66
Cg -Cm	21.73	4.76	21.85	4.85	0.24	0.54	0.70	2.49
Pg -Pm	31.62	3.10	31.76	3.09	0.00	0.22	0.26	0.68
Ag-Pg	30.19	3.18	27.13	4.68	0.00	3.28	3.78	11.44
Am-Pm	22.00	2.63	25.60	5.17	0.00	3.41	3.90	14.31
Dm-Cm	13.84	2.25	14.80	2.45	0.00	0.80	1.06	5.60
Dg-Cg	15.10	2.34	15.33	2.25	0.04	0.68	0.76	4.45

All values are mm
MAD: mean absolute difference
TEM: Technical error of measurement
REM: relative error magnitude
p values from paired Student's t tests. All p values are significant, $p < 0.05$, except Cg-Cm distance.